

Article

Modifying Headspace Sampling Environment Improves Detection of Boar Taint Compounds in Pork Fat Samples

Clément Burgeon ¹, Alice Markey ², Yves Brostaux ³ and Marie-Laure Fauconnier ^{1,*}

- ¹ Laboratory of Chemistry of Natural Molecules, Gembloux Agro-Bio Tech, Université de Liège, Passage des Déportés 2, 5030 Gembloux, Belgium; cburgeon@uliege.be
- ² Laboratory of Numerical Genetics Genomics and Modelling, Gembloux Agro-Bio Tech, Université de Liège, Passage des Déportés 2, 5030 Gembloux, Belgium; alice.markey@uliege.be
- ³ Statistics, Informatics, and Applied Modeling Unit, Department of AgroBioChem, Gembloux Agro-Bio Tech, Université de Liège, Passage des Déportés 2, 5030 Gembloux, Belgium
- * Correspondence: marie-laure.fauconnier@uliege.be

Abstract: The extraction of boar taint compounds from pork fat samples was performed under various temperature (150, 300 and 450 °C) and atmosphere (air, nitrogen and reduced pressure) conditions. This aimed at understanding which conditions allow the greatest extractions of indole, skatole and androstenone (present in backfat in low concentrations) while limiting the presence of other VOCs in the headspace of heated fat (interfering with correct VOC-based detection of boar taint compounds). Indole and skatole were extracted in the greatest concentrations when heating backfat at 450 °C under reduced pressure, while androstenone was highest when heating at 300 °C under reduced pressure. Oxidation products were most abundant under air conditions, nitrogenated products appeared in the presence of a nitrogen-enriched atmosphere, and lastly, molecules intrinsic to boar fat saw their headspace concentration increase with reduced pressure. The combination of 450 °C and reduced pressure atmosphere was suggested for the heating of backfat prior to detection with analytical methods and to complement the current sensory analysis.

Keywords: boar taint detection; headspace solid phase microextraction; vacuum-assisted solid-phase microextraction; nitrogen-assisted solid-phase microextraction; pork



Citation: Burgeon, C.; Markey, A.; Brostaux, Y.; Fauconnier, M.-L. Modifying Headspace Sampling Environment Improves Detection of Boar Taint Compounds in Pork Fat Samples. *Chemosensors* **2023**, *11*, 551. <https://doi.org/10.3390/chemosensors11110551>

Academic Editors: Bruno Medronho and María José Aliaño-González

Received: 31 August 2023

Revised: 19 October 2023

Accepted: 24 October 2023

Published: 28 October 2023



Copyright: © 2023 by the authors. Licensee MDPI, Basel, Switzerland. This article is an open access article distributed under the terms and conditions of the Creative Commons Attribution (CC BY) license (<https://creativecommons.org/licenses/by/4.0/>).

1. Introduction

Boar taint is an unpleasant odor found in the meat of some uncastrated pigs that is released upon its cooking. This odor is due to a complex set of molecules that are stored in fat. Several molecules have been cited as contributing to this odor (including indole, α - and β -androstenol, and 2-aminoacetophenone, amongst others). However, two molecules have been found to be the major elements responsible for this odor: androstenone and skatole, which give, respectively, a strong urine and fecal odor to the meat [1–4].

To reduce the risk of occurrence of boar taint in pigs, surgical castration of male piglets is used. This can be accomplished with anesthesia or analgesia but is, however, frequently performed without any pain relief [5]. Given evident animal welfare issues, an intent declaration was written in 2010 to abandon surgical castration without pain relief in the European Union by the 1st of January 2018, provided that viable alternatives are offered [6]. Several alternatives have been suggested, and three realistic alternatives stand out: surgical castration with pain relief, production of entire males (i.e., no castration) and immunocastration (i.e., testicular functions are deactivated through the neutralization of the hypothalamic–pituitary–gonadal axis hormones) [7]. Although immunocastration is said to have high success rates in the prevention of boar taint [8], carcasses with boar taint can still occur [9]. Whatever the alternative used, the tainted carcasses must be discriminated from untainted ones.

The discrimination of carcasses based on their taint is often performed in slaughterhouses, either at-line or on-line. Currently, two methods are used. The first one is the sensory evaluation of boar taint performed by a human nose, which smells the carcasses' backfat after having heated it [10]. The second one is a colorimetric method, which gives results in skatole equivalents [11]. Given evident flaws with the first method due to human error and incomplete information with the second (analysis of indolic compounds only), researchers have been investigating other detection methods.

Although several methods have been tested throughout the years [12], few methods seem promising in the near future: laser diode thermal desorption–tandem mass spectrometry (LDTD-MS/MS), which is already being tested in Danish slaughterhouses [13], rapid evaporative ionization mass spectrometry (REIMS) [14] and RAMAN spectroscopy [15,16]. These last two methods could be easily implemented for on-line use in slaughterhouses given the possibility of being hand-held tools. Other promising technologies for on-line application include all analytical methods based on the detection of volatile organic compounds (VOCs) present in the headspace of heated fat. These are at the heart of several current ongoing studies and include, for example, VOC sensor-based methods and portable gas chromatography–mass spectrometry (GC-MS) [12].

Boar taint compounds are strongly lipophilic and are hard to volatilize (vapor pressures of 7.3×10^{-4} kPa and 1.3×10^{-6} kPa at 25 °C for skatole and androstenone, respectively). Therefore, regardless of the VOC-based method used (i.e., sensory analysis or analytical methods based on headspace VOC detection), fat must be heated at high temperatures to ensure that boar taint compounds are present in the headspace and subsequently detectable. Several works have already tested variable heating temperatures. The heating temperature of 400 °C was considered as the optimal one for the extraction of boar taint compounds in a study where temperatures were varied from 100 °C to 400 °C [17]. The impact of heating temperatures 150 °C and 180 °C were also investigated on the release of skatole and androstenone and on general VOC profiles [18]. In this study, it appears that skatole and androstenone were released in low concentrations from the fat and that a variety of molecules, such as fatty acids, aldehydes, ketones and alcohols, were generated as products of lipid oxidation occurring at high temperatures [18]. Lastly, 120 °C was also tested to heat backfat and it also appeared in this case that aldehydes and fatty acids were generated when heating pork fat at this temperature [19]. These molecules could hamper the correct detection of the targeted compounds given sensor fouling in the case of VOC-based sensors, and greater saturation of the human nose in the case of sensory evaluation.

To facilitate the detection of boar taint compounds by limiting the production of oxidation products, the use of high temperatures could be combined with an oxygen-deprived sampling environment. Such environments can be produced in different ways. Firstly, air present in the sampling headspace can be partially replaced by another gas. Secondly, the sample's headspace can be air-evacuated, thereby creating a reduced pressure atmosphere. Such reduced pressure atmosphere has already been investigated for the headspace extraction of several analytes to accelerate their extraction kinetics. It has been found that volatilization rates are greater in such reduced pressure atmosphere environments, having a direct impact on the amount of analytes extracted in non-equilibrium conditions [20].

In this study, we have therefore analyzed the impact of increased temperature and a modified sampling environment on boar taint compounds' extraction. This was performed with a unique experimental device which allows to perform dynamic headspace solid phase microextraction (dynamic HS-SPME) under modified atmospheres.

To the best of our knowledge, this study is the first to adapt the sampling atmosphere to supplement the elevated heating temperature in the framework of boar taint detection. In this study, results both for known boar taint compounds and for other VOCs extracted from the fat matrix or generated when heating the fat were gathered.

The objective of this research was to determine the optimal conditions for boar taint compound extraction. This means understanding which combination (1) gives maximum

headspace concentration of boar taint compounds and simultaneously (2) results in minimum extraction and production of other VOCs. Subsequently, the use of such parameters for VOC-based boar taint detection was discussed. These parameters were discussed for (1) analytical methods based on headspace detection of VOCs, such as sensor-based and GC-MS based techniques, and (2) for sensory evaluation of this taint.

2. Materials and Methods

2.1. Samples

Sow fat ($n = 5$) and tainted boar fat ($n = 11$) were collected from a local slaughterhouse. The sow fat was randomly selected. The tainted boar fats, on the other hand, were selected after these had been tested for boar taint by a trained assessor through the human nose method. The collected samples were frozen at $-20\text{ }^{\circ}\text{C}$ at the slaughterhouse, transported in a cooler and stored again at $-20\text{ }^{\circ}\text{C}$ until further analyses. The presence of boar taint was validated through the quantification of skatole and androstenone in fat by high-performance liquid chromatography fluorescence detection (HPLC-FD), which is described later in this section.

2.2. Sample Characterization

2.2.1. Skatole and Androstenone Quantification in Backfat

Skatole (Figure 1a) and androstenone (Figure 1b) quantification were performed with a high-performance liquid chromatography fluorescence detection (HPLC-FD) method adapted and described by Burgeon, Markey et al. (2021) [18].

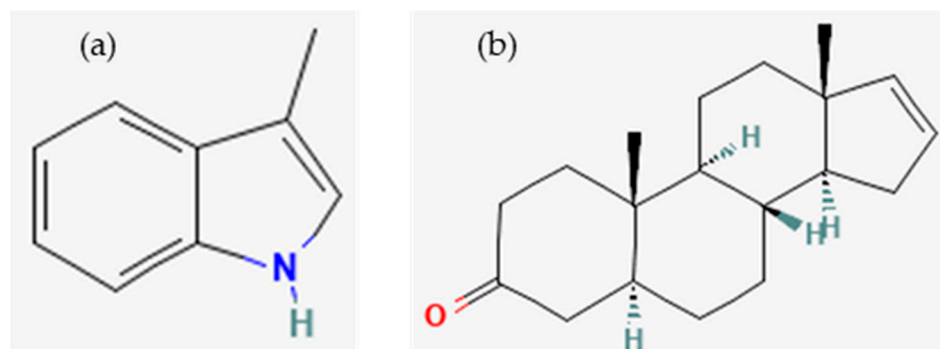


Figure 1. Molecular structure of (a) skatole and (b) androstenone [21,22].

Briefly, 0.5 g of backfat was homogenized with methanol (total of 3 mL) by using an Ultra-Turrax (total run time of 2 min at 13,500 rpm). The sample was ultrasonicated (5 min) and placed in an ice bath (15 min) prior to centrifugation at 7700 rpm at $4\text{ }^{\circ}\text{C}$. The supernatant was then filtered on a $0.45\text{ }\mu\text{m}$ filter paper, and $140\text{ }\mu\text{L}$ was put in a vial for analysis.

The sample was then derivatized automatically with the autosampler ($30\text{ }\mu\text{L}$ of 2% dansylhydrazine in methanol, $4.4\text{ }\mu\text{L}$ of water and $10\text{ }\mu\text{L}$ of 20% *v/v* BF_3). Through this reaction, androstenone reacts with dansylhydrazine to produce fluorescent dansyl derivatives, i.e., dansylhydrazones (Figure 2) detectable through fluorescent detection [23,24]. The reaction was performed for 5 min, and $20\text{ }\mu\text{L}$ was then injected into the HPLC to be later detected with the fluorescent detector (details on the HPLC-FD parameters are described in a previous research paper [18]).

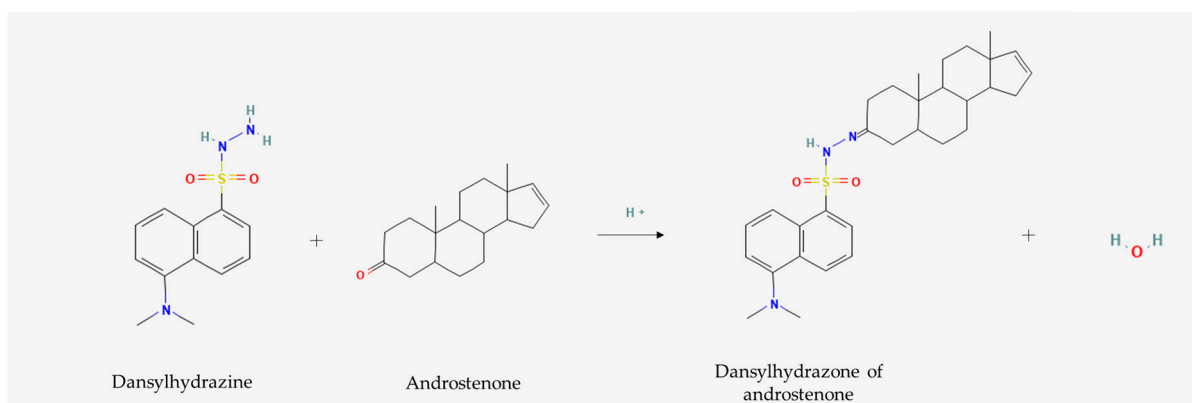


Figure 2. Reaction of dansylhydrazine with androstenone to form a fluorescent derivative (dansylhydrazone of androstenone) (molecular structures issued from PubChem [21,25]).

Boar fat is considered tainted if the skatole or androstenone concentrations are above the thresholds of 200 ng g^{-1} of fat or 1000 ng g^{-1} of fat, respectively [18].

2.2.2. Fatty Acid Composition Analysis

The fatty acids were quantified as fatty acid methyl esters (FAMES) based on a previously described method [26].

Briefly, 10 mg of melted pork fat sample were added to 0.2 mL of hexane and 0.5 mL of BF_3 reagent (methanol/ BF_3 14%/hexane (55:25:20)), which was then heated to $70 \text{ }^\circ\text{C}$ in a water bath for 1.5 h. The FAMES were extracted by adding 0.5 mL of a NaCl-saturated solution, 0.2 mL of 10% H_2SO_4 first stirred and 8 mL of hexane added.

After vigorous shaking of the tube, $0.5 \text{ }\mu\text{L}$ of the top layer of the solution was injected in cold on-column mode into the capillary column ($30 \text{ m} \times 250 \text{ }\mu\text{m} \times 0.25 \text{ }\mu\text{m}$, CP9205 VF-WAX, Agilent Technologies Inc., Santa Clara, CA, USA) of the GC system (6890A, Agilent Technologies Inc., Santa Clara, CA, USA). Helium was used as a carrier gas at $1.234 \text{ mL min}^{-1}$. The oven temperature program was as follows: start at $50 \text{ }^\circ\text{C}$ for 0.5 min, increase by $30 \text{ }^\circ\text{C min}^{-1}$ up to $150 \text{ }^\circ\text{C}$, and then increase by $5 \text{ }^\circ\text{C min}^{-1}$ up to $250 \text{ }^\circ\text{C}$ and hold for 10 min.

The FID detector parameters were as follows: temperature of $250 \text{ }^\circ\text{C}$, helium flow rate of 30 mL min^{-1} , air flow rate of 400 mL min^{-1} and a N_2 makeup flow rate of 25 mL min^{-1} . Individual FAMES were identified by retention times with reference Supelco[®] 37 Component FAME Mix (47885-U Sigma Chemical Co., St. Louis, MO, USA).

2.3. Variation of the Sampling Parameters on VOC Extraction from Fat

2.3.1. Studied Parameters

Heating of the sow ($n = 5$) and boar ($n = 11$) backfat samples was performed with nine different temperature–atmosphere combinations. Three temperatures (150 , 300 and $450 \text{ }^\circ\text{C}$) and three different atmospheres (air, nitrogen and a reduced pressure atmosphere) made up the nine combinations. Each combination was tested on each fat sample in a completely randomized design. The choice of the selected atmospheres was previously explained in the introduction. Regarding the choice of temperatures on the other hand, $150 \text{ }^\circ\text{C}$ was selected, as it had been previously tested in another research study, only under normal air conditions, but would, however, allow some comparison to it [18]. The temperature of $450 \text{ }^\circ\text{C}$ was selected, as it is the maximal temperature of most commercial soldering irons frequently used to detect boar taint [27,28]. Studying this temperature would therefore give an idea of the VOCs if the researchers were to develop a similar sampling apparatus but with a soldering iron. Lastly, $300 \text{ }^\circ\text{C}$ was selected, as it is the intermediate temperature.

2.3.2. Heating Device Description

The above-mentioned sampling conditions were tested with an in-house developed device. This apparatus is composed of the VOC extraction device to which various tubing are connected to allow dynamic extraction of the produced VOCs.

The VOC extraction device consists of two separate parts: a silicone plate with the heating system (Figure 3a), which is found inside a reinforced 3D-printed enclosure (Figure 3b,c, PET-G 3D printer filament, RS-PRO, London, UK).

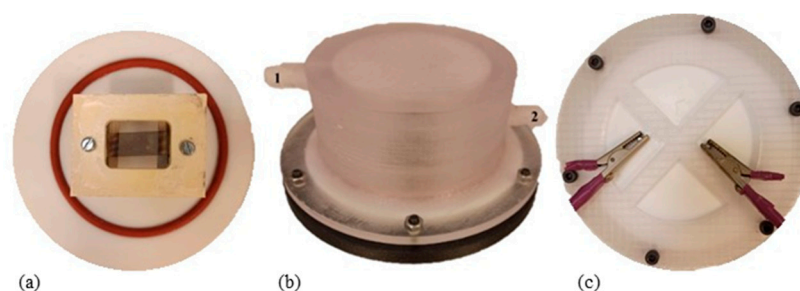


Figure 3. (a) Top view of the heating device. (b) Side view of the 3D printed enclosure, with entry and exit port (1 and 2) to allow the flow of air and nitrogen. (c) Bottom view with connections to the power supply. The headspace volume inside the enclosure is approximately 150 mL (cylinder is 6.5 cm wide and 4.5 cm high).

The silicone plate is equipped at its center with a heating resistance (Ni80 Mesh Wire, Vandy Vape, MI, USA), under which the fat is positioned. An O-ring is integrated to the silicone plate to ensure better closing with the 3D-printed enclosure.

The enclosure was 3D-printed (MK3S+ 3D printer, Prusa, Prague, Czech Republic), and was then subjected to an annealing process to reinforce it and make it more gas-proof. The annealing was performed as follows: in a Pyrex container, the 3D print was dipped and covered in crushed NaCl. The device was then put in a heat chamber (UFB 500, Memmert GmbH, Schwabach, Germany) set at 120 °C. Once the salt and 3D print reached this temperature, it was left in the heat chamber for 3 h. After leaving the Pyrex container at room temperature overnight, the reinforced 3D print was taken out of the salt.

The 3D-printed enclosure is equipped with nuts and bolts to further seal the device during sampling. The heating resistance is linked to a bench power supply (CPX200DP, Aim-TTi, Cambridgeshire, UK) using crocodile clips attached to both of its ends (Figure 3c).

Lastly, the VOC extraction device has two ports on the sides (1 and 2 in Figure 3b) to allow a flow of air or nitrogen or to create reduced pressure conditions. In the case of air and nitrogen conditions, the gas is pushed through the device (Figure 4a). In the case of reduced pressure, air is pulled out of the extraction device by using a vacuum pump (E2M2, dual-stage vacuum pump, Edwards) (Figure 4b).

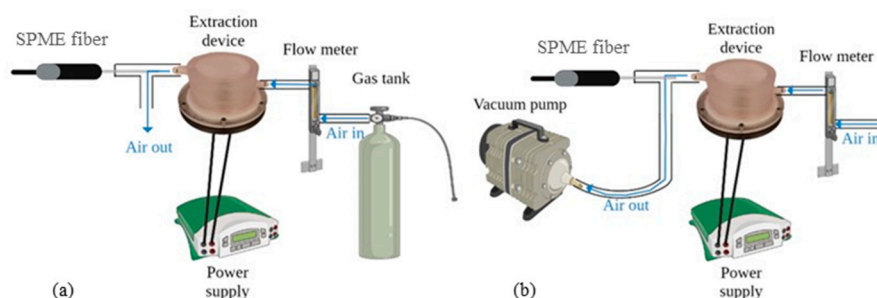


Figure 4. Arrangement depending on the atmosphere tested. (a) Air and nitrogen are pushed through the device; (b) air is pulled to reduce the pressure inside the device.

2.3.3. Extraction Parameters for Heating of Fat and VOC Sampling

The backfat samples were prepared by cutting two cylindrical pieces 1 cm in diameter and 2 cm high from a larger backfat piece. These samples were placed under the heat resistance, and the device was sealed. The device was then connected to the bench power supply using crocodile clips and connected to the gas bottles or the vacuum pump depending on the tested modality.

In both cases, the gas flow rate was fixed at 200 mL min^{-1} . Once the gas passed through the device for 2 min, the sampling took place. The polydimethylsiloxane (PDMS) 100 μm fiber (Supelco) was put in the sampling port, and the bench power supply was turned on at a specific power (determined earlier with the use of a multimeter and thermocouple) to ensure that temperatures of 150, 300 or $450 \text{ }^\circ\text{C}$ were attained. Heating of the fat samples and VOC sampling with the PDMS fiber took place simultaneously for 5 min with a flow rate of 200 mL min^{-1} maintained throughout the process.

The sampling device was cleaned with hexane between each analysis.

2.3.4. SPME-GC-MS VOCs Analyses

Analyses were performed by GC-MS (7890A-5975C, Agilent Technologies Inc.) equipped with an HP-5 MS capillary column ($30 \text{ m} \times 250 \mu\text{m} \times 0.25 \mu\text{m}$, Agilent Technologies Inc.). SPME fiber desorption took place at $250 \text{ }^\circ\text{C}$ for 2 min. This was followed by a manual conditioning of the fiber between each analysis at $250 \text{ }^\circ\text{C}$ for 15 min. Helium was used as a carrier gas at a flow rate of 1.2 mL min^{-1} . The oven temperature program was as follows: starting at $40 \text{ }^\circ\text{C}$ with a hold for 2 min, then increase by $5 \text{ }^\circ\text{C min}^{-1}$ up to $250 \text{ }^\circ\text{C}$, followed by an increase by $15 \text{ }^\circ\text{C min}^{-1}$ to $300 \text{ }^\circ\text{C}$ with a hold for 5 min (total run time of 52.33 min). The mass spectrometer was set to have a temperature of $230 \text{ }^\circ\text{C}$ at the ion source and $150 \text{ }^\circ\text{C}$ at the quadrupole. The mass spectrometer was programmed with a SIM/SCAN acquisition mode. In SCAN mode, the mass spectra were scanned from 35 to 500 amu. In SIM mode, the targeted ions were 117 for indole, 130 for skatole and, lastly, 272 for androstenone. The peak area from these ions was analyzed to establish the response curves, as mentioned in the section below. The pure standards of indole (CAS n° 120-72-9, Sigma Aldrich, Darmstadt, Germany), skatole (CAS n° 83-34-1, Sigma Aldrich, Darmstadt, Germany) and androstenone (CAS n° 18339-16-7, Sigma Aldrich, Darmstadt, Germany) were injected to ensure the correct identification of these molecules.

2.4. Statistical Analysis

A principal components analysis (PCA) was performed on the VOC data to detect the existing trends among the different samples. The normalized (scaled to unit variance) peak areas were used for the PCA. This was conducted in R (R 4.0.2 software, R Development Core Team, Boston, MA, USA). One-way and two-way ANOVA (two fixed factors: temperature and atmosphere) were performed with Minitab software version 19.1 (Minitab Inc., State College, PA, USA). The gathered results for the specific analysis of boar taint compounds in the boar fats were used to generate response curves based on a quadratic fit model. The response for this model is the peak area of the compounds of interest and the inputs are the block effect resulting from the analysis of 11 backfats from distinct individuals, the linear and quadratic effects of the heating temperature (quantitative variable) and, lastly, the sampling atmosphere (qualitative variable). The individual plots and temperature-dependent curves of the PCA were generated in R. All the other graphs and tables were developed in Excel (Microsoft Office 2016).

3. Results

3.1. Characterizing the Fat Samples—Fatty Acid Composition and Boar Taint Compounds' Content Analyses

Prior to the analysis of the VOC profiles obtained under the different temperature–atmosphere combinations, the backfat samples were characterized. Even though this was

not the main aim of the study, this was briefly performed to ensure that no abnormal trend in terms of the fatty acid composition was present and that all the boar backfat was tainted.

The fatty acid composition was analyzed for both boar and sow fats (Appendix A). Monounsaturated fatty acids (MUFA) were the most abundant, followed by saturated fatty acids (SFA) and, lastly, by polyunsaturated fatty acids (PUFA). In terms of the individual fatty acids, the three most abundant compounds were *cis*-C18:1*n*-9, followed by C16:0 and *cis*-C18:2*n*-6 (Figure 5). It appears, from the obtained results, that the trends observed throughout the data are similar to those found in previous studies [29], both in terms of the fatty acid classes and the specific fatty acids constituting them.

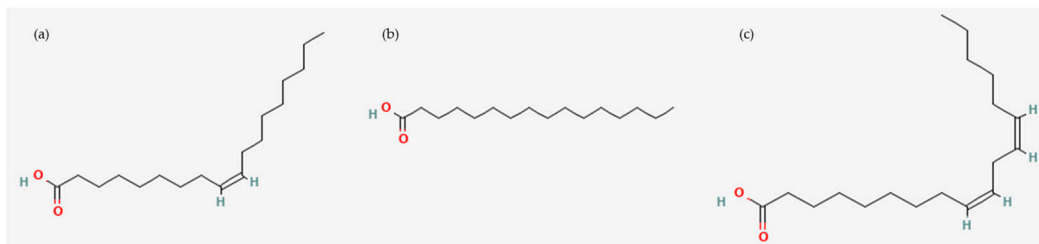


Figure 5. Molecular structure of (a) (Z)-octadec-9-enoic acid (*cis*-C18:1*n*-9), (b) hexadecenoic acid (C16:0) and (c) (9Z,12Z)-octadeca-9,12-dienoic acid (C18:2*n*-6) [30–32].

The skatole and androstenone contents were also analyzed for boar backfat to ensure that these were tainted (Appendix B). The sow fats were not analyzed for skatole and androstenone content, as these do not develop boar taint (as verified in a previous research [18]). In fact, skatole's higher content in boar fat is linked to testicular steroids production. The latter has an inhibiting effect on CYP2E1, the main enzyme involved in skatole's metabolism. In the absence of testicular steroids, skatole metabolism functions correctly and therefore does not accumulate [33].

All the boar fats selected either had skatole or androstenone concentrations above the thresholds of 200 ng g⁻¹ of fat and/or 1000 ng g⁻¹ of fat, respectively. These are rejection thresholds frequently used to distinguish tainted from untainted samples through analysis of these molecules' content in fat [18,34].

3.2. Impact of Sampling Parameters Variations on Boar Taint Compounds Headspace Sampling

High temperatures have always been used to heat pork fat for sensory evaluations of boar taint, given that boar taint compounds are known to be highly lipophilic and possess low vapor pressure (7.3×10^{-4} kPa and 1.3×10^{-6} kPa at 25 °C for skatole and androstenone, respectively) [18]. These temperatures usually range from approximately 60 °C with a microwave treatment [35] to 240 °C with a soldering iron [36], although intermediate temperatures of 150/180 °C are frequently used [18,28]; however, temperatures higher than 240 °C have also been tested for other headspace-based detection techniques. In fact, in a study aiming at developing a new rapid SPME-GC-MS method for boar taint detection, the extraction parameters were optimized. Temperatures ranging from 100 °C to 400 °C were tested, and the optimum temperature appeared to be 400 °C for the extraction of indole, skatole and androstenone under normal atmospheric conditions [17].

In the present study, we analyzed VOC profiles obtained when heating pork fat with temperatures ranging from 150 °C to 450 °C under three different sampling atmospheres (air, nitrogen and reduced pressure). As a reminder, the data were acquired in SIM/SCAN mode during the GC-MS analysis of each sample. The SIM data were obtained for boar taint specific compounds, as these are present in low concentrations. This should help in solving the first part of the objective, i.e., understanding what temperature-atmosphere combination gives the maximum headspace concentration of boar taint compounds. The SCAN data were obtained for all the other VOCs, which are not necessarily responsible for boar taint. This should help in answering the second part of the objective,

i.e., understanding what combination results in minimum extraction and production of other VOCs.

Several molecules have been suggested to contribute to boar taint along with androstenone and skatole. These molecules include 2-aminoacetophenone, which is linked to the synthesis and metabolism pathway of skatole; androstadienone, 3 α - and 3 β -androstenol linked to androstenone's synthesis and metabolism; and, lastly, other molecules for which the link to androstenone and skatole are less evident [3,4]. However, skatole and androstenone remain the major responsible molecules for this odor. Taken together, these two compounds account for 50% of the variation in boar taint [37]. Additionally, a third molecule often analyzed with skatole and androstenone is indole. In fact, it is recognized as playing an important role in boar taint [2,38].

In this study, temperature-dependent curves were performed for these three main contributors to boar taint. Three curves are displayed each time, representing, respectively, the sampling under air, nitrogen and reduced pressure atmosphere (Figure 6).

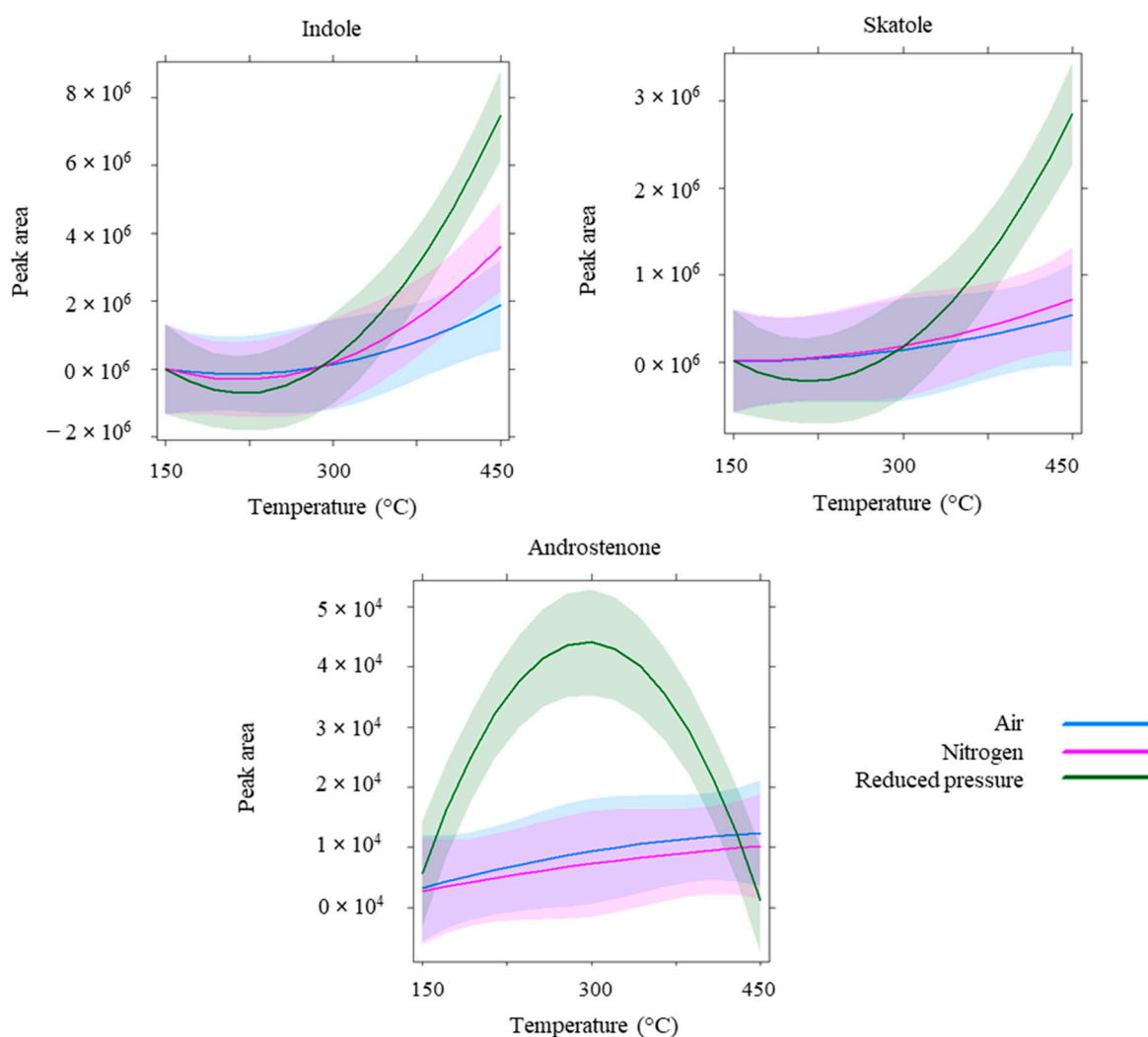


Figure 6. Response curves for boar taint compounds (indole, skatole, and androstenone) depending on the sampling parameters. For each compound, three curves are drawn for each sampling atmosphere: blue = air, pink = nitrogen and green = reduced atmosphere. The *y*-axis represents peak area of the analyzed compound, and the *x*-axis represents heating temperature. Confidence bands are represented each time to allow for easy graphical visualization of the significance of the results, i.e., an overlap of the bands indicates that no significant difference is observed.

From Figure 6, it can be noticed that the three studied molecules do not follow the same trend. The first behavior observed is that of indole and skatole. In these response curves, a general tendency to increase extraction of the molecules of interest with a temperature of 450 °C and by modifying the atmosphere is perceived. At 450 °C, peak areas of the molecules of interest increased for nitrogen atmosphere (although not significantly different from the air atmosphere) and are the highest for the reduced pressure atmosphere conditions (significantly different from the two other atmospheres).

The second observed behavior is the one exhibited by androstenone. From its response curves, it can be observed that the extraction yield is significantly higher when heating fat samples at 300 °C under reduced pressure conditions. In a previous research paper which studied extraction temperatures ranging from 100 °C to 400 °C under normal air conditions, it was found that 400 °C is the optimal temperature [17]. Similar behavior is expected in the present case for androstenone, i.e., a general increase from 150 to 450 °C. The lower headspace concentrations observed under reduced pressure at 450 °C could be explained by the greater headspace concentrations of other semi-volatile organic compounds at 450 °C under reduced pressure compared to nitrogen and air atmospheres (discussed later in this section). This leads to competitive adsorption on the SPME fiber, which is a real challenge in the case of complex samples, such as the backfat used here. In fact, components present in high concentrations can displace minor components from the fibers' surface [39]. Lastly, when observing Figure 6, one can see that a minimum headspace concentration is found with the combination of 225 °C under reduced pressure for indole and skatole. Given the clear overlap of the confidence intervals at 225 °C when comparing the different atmospheres, one can understand that this decrease is not significant and is simply explained by the choice of the model used (quadratic linear model).

Many other VOCs, which are not directly responsible for boar taint, constitute the profiles obtained when heating fat with the different temperature–atmosphere parameters. A total of 193 compounds were found in a large diversity of families (Appendix C). Amongst these are found 30 aldehydes, 10 alcohols, 17 alkanes, 11 fatty acids, 18 benzene derivatives and 22 ketones typically found in VOC profiles of heated fat [18,40]. Other less usual chemical families, however, were also found. These include heterocyclic compounds (such as pyridines) and other nitrogenated compounds (nitriles, amines and amides).

Given the amount of information present for the VOC profiles, a PCA was performed to point out trends among the samples. This PCA was performed on the peak area data to take into account the differences existing in terms of the overall VOC abundance between the different modalities. As mentioned in the introduction, it is believed that nitrogen and a reduced pressure atmosphere could have an impact on generated VOC profiles by limiting the presence of lipid oxidation products. To verify this through fast visualization of the PCA, the analyzed samples were labeled based on their sampling atmosphere (Figure 7). It is worth noting that no distinction was observed in general VOC profiles based on the fat type (Appendix D). This concurs with the observations made on the general VOC profiles in a previous study performed by the authors of this paper [18]. Both boar and sow fats were used for the following PCA, as they have been confronted with the same sampling conditions, and although no distinction is observed based on the fat type, a distinction can still be observed based on the sampling conditions.

From Figure 7, which is an individuals' plot taking into account approximately 38% of the total variance in the data, several observations are evident. Firstly, when looking at principal component 1 (PC1), it can be noticed that the VOC profiles obtained under the nitrogen and reduced pressure atmosphere conditions tend to accumulate on the left-hand side of this PC, while the VOC profiles obtained under the normal air atmosphere tend to spread along the right side of PC1 (going towards the more positive values of PC1).

A second noticeable trend is found along principal component 2 (PC2). Firstly, the reduced pressure atmosphere samples tend to aggregate close to the center of this PC with a slight tendency towards positive PC2 coordinates. Secondly, one can observe that the nitrogen samples tend to spread along positive PC2 values. Lastly, with the exception

of one sample (number 32) with a high PC2 coordinate, all the other air samples either have low positive PC2 coordinates or negative coordinates. There are also intra-group variations. This is particularly true in the case of the air samples, in which two main trends are observed, i.e., those mainly oriented along PC2 and those mainly spreading along PC1. This is due to the varying sampling temperatures (e.g., samples 74, 92 and 147 were sampled at 300 °C, while samples 86, 50 and 121 were sampled at 450 °C).

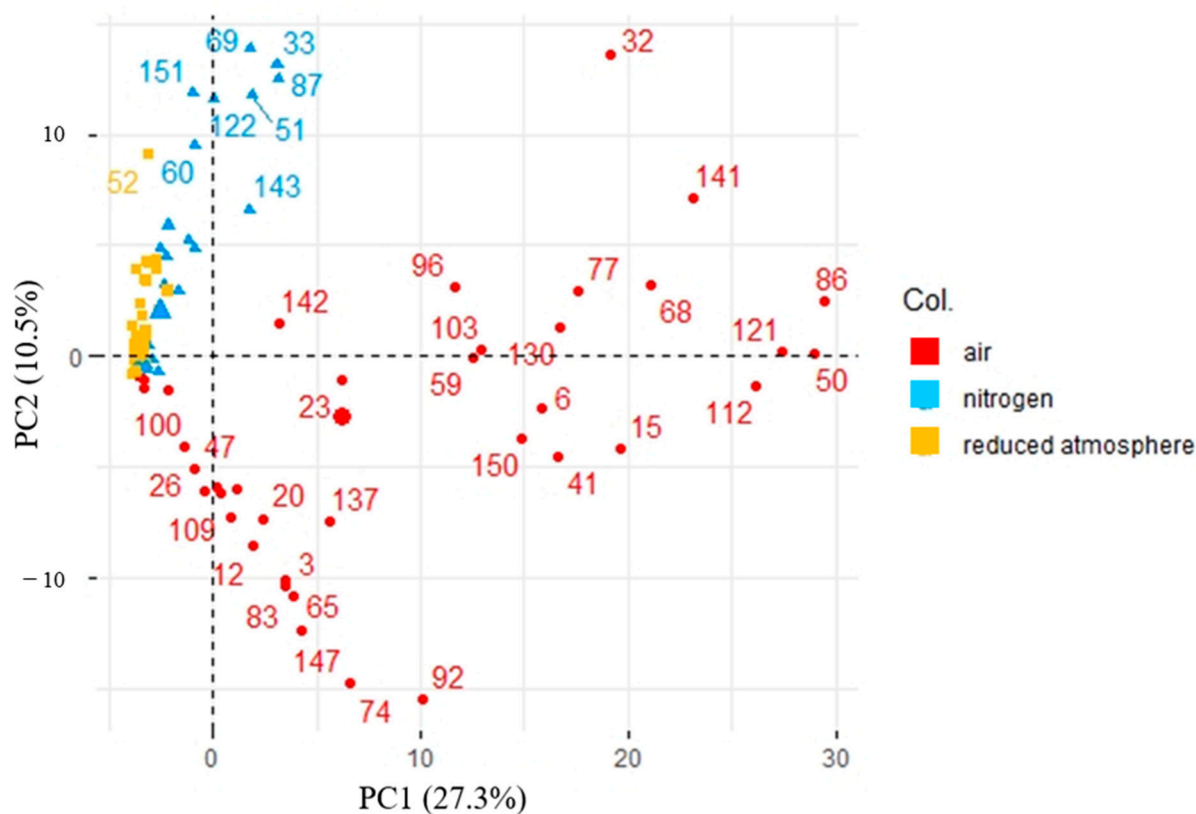


Figure 7. Principal component analysis individual plot comparing backfat samples based on their VOC profiles. Samples are labeled based on the atmosphere in which the VOCs were sampled: yellow, reduced pressure atmosphere; blue, extraction in a nitrogen atmosphere; red, extraction under normal air atmosphere. Normalized peak areas were used for this PCA.

These observations imply that the diversity of the VOCs found in the reduced pressure atmosphere profiles is much lower than in the nitrogen and air VOC profiles. Secondly, the different directions taken by the air and nitrogen VOC profiles (air along PC1 and nitrogen along PC2) imply that the molecules that constitute them are very different.

To understand which molecules are at the origin of these differences, an analysis of the correlation of each VOC to both PCs was performed. Although many are significantly correlated to these PCs, only the top 10 molecules with the greatest correlation were investigated (Table 1).

For PC1, four of the top ten VOCs most correlated to PC1 are aldehydes. This is not surprising, as aldehydes are typical oxidation products produced when heating fat in an unaltered atmosphere at a high temperature (e.g., heptanal, decanal and octanal are oxidation products of (Z)-octadec-9-enoic acid [41]). In fact, several studies have already reported aldehydes as a major chemical class constituting VOC profiles of heated fat [18,40]. Alkanes, such as undecane and tridecane, are also products of lipid oxidation.

Table 1. Top 10 contributors for principal component 1 (left) and top 10 contributors for principal component 2 (right). All correlations very highly significantly correlated to PC 1 and 2 ($p < 0.001$).

PC1		PC2	
VOC Considered	Correlation	VOC Considered	Correlation
undecane	0.96	3-phenylpropanenitrile	0.69
heptanal	0.95	Pyridin-2-amine	0.63
butylbenzene	0.94	3-methyl-1H-pyrrole	0.63
decanal	0.94	2,5-dimethyl-1H-pyrrole	0.63
octanal	0.94	2-phenylacetoneitrile	0.62
propylbenzene	0.92	2,5-dimethylpyridine	0.60
(E)-oct-2-enal	0.92	2,3,4-trimethyl-1H-pyrrole	0.56
tridecane	0.92	1-phenylpropan-2-one	0.55
pentylbenzene	0.90	2-methyl-1H-pyrrole	0.54
non-1-ene	0.89	4-ethyl-2-methyl-1H-pyrrole	0.52

The VOCs presented as the most correlated to PC2, however, are less common in research focusing on VOC profiles of heated fat specifically. Out of the 10 molecules mentioned as strongly correlated to PC2, 7 are pyrroles and pyridines, which are found in some air VOC profiles but remain, however, much more present in the nitrogen VOC profiles. Observing these as characteristic of VOC profiles obtained under nitrogen atmospheres does not come as a surprise, as these are typically produced during the pyrolysis (i.e., reaction at extremely elevated temperature in an inert atmosphere) of amino acids [42]. The amino acids being degraded here originate from the connective tissue making up the fat matrix.

As mentioned earlier, when looking at the PCA in Figure 7, it appears that all the reduced pressure atmosphere samples are gathered together close to the center of PC2 and on the left side of PC1. The diversity of molecules for these samples is much smaller. In fact, 80 VOCs were identified in the reduced pressure atmosphere samples, as opposed to 146 and 162 for the nitrogen and air atmospheres, respectively.

However, several molecules were exclusively found in the reduced pressure atmosphere profiles (Appendix C). These are methyl hexadecanoate, methyl octadecanoate, nonanoic acid, decanoic acid, dodecan-6-ylbenzene and pyridine-2-carboxamide. With the exception of dodecan-6-ylbenzene and pyridine-2-carboxamide, all the other molecules mentioned here are fatty acids or methyl esters of fatty acids. These molecules are extremely lipophilic and possess very low vapor pressures (e.g., methyl octadecanoate has a vapor pressure of 1.813×10^{-6} at 25 °C [43]). In other words, under normal atmospheric pressure, the extraction rates of such analytes from a fat matrix and, consequently, the time required to reach equilibrium between the sample and the SPME fiber will be very long. Several factors, however, can improve the extraction rate. Amongst these is the reduction of the sampling pressure, as previously demonstrated on various matrices, such as on olive oil [44]. Finding these molecules exclusively in the headspace of the reduced pressure atmosphere samples further supports the findings on the acceleration of the extraction rates with reduced pressure atmosphere conditions.

Similarly, several molecules were observed in all three sampling atmospheres but were found in much greater abundance in the VOC profiles of the reduced pressure atmosphere conditions. This is particularly true for the semi-volatile organic compounds found at the end of the chromatographic analysis, such as octadecanoic acid and squalene found in significantly higher concentrations under reduced pressure as opposed to the air and nitrogen profiles at 450 °C ($p < 0.01$).

These observations concur with previous findings. The extraction rates under non-equilibrium conditions have been previously found to improve with reduced pressure atmosphere sampling, and in particular for semi-volatiles [20].

4. Discussion

Considering both VOC profiles as a whole and the boar taint compounds specifically, it appears from our data set constituted of 16 fat samples that 450 °C under reduced pressure atmosphere is the best sampling condition for maximum headspace concentrations of boar taint compounds with minimum extraction and production of other VOCs. A greater number of samples could be tested in these conditions, however, to validate these findings.

In this study, the highest extraction yields were obtained for indole and skatole under these conditions. Although androstenone was found in greater headspace concentrations at 300 °C, favoring 450 °C rather than 300 °C as the heating temperature seems justified, as skatole has a stronger contribution to boar taint than androstenone. In fact, a correlation of 0.69 between the human nose score (HNS) attributed during a sensory evaluation and skatole, and a correlation of 0.42 between HNS and androstenone has been previously determined [45]. Similarly, consumer dissatisfaction for the odor of entire male pork has been demonstrated to be more associated with high levels of skatole than androstenone [46]. Using 450 °C implies extracting more skatole and, in turn, obtaining a better representation of boar taint than if a temperature of 300 °C was used.

Adapting the sampling environment leads to the reduction of oxidation products in the headspace, even at extremely high temperatures (such as 450 °C). Even if reduced pressure leads to increased extraction of fat-intrinsic compounds, this sampling atmosphere seems interesting to use for several VOC-based detection methods.

At first glance, a nitrogen atmosphere could be considered a viable alternative for some sensor-based VOC methods. In fact, the sensitive layer of some sensors is made up of polypyrroles [47]) and might therefore be less sensitive to pyrrole derivatives produced in this case. This remains, however, a case-specific hypothesis and is most probably not true for other sensor technologies. A reduced atmosphere, therefore, seems the best atmosphere to use for sensors. In fact, although a greater abundance of these fatty acid derivatives might lead to greater detector fouling, the overall smaller diversity of compounds observed in the headspace might help in working on specific solutions to reduce their interferences.

For other analytical methods, such as the portable SPME-GC-MS [17], reduced pressure and heating at 450 °C is also the best combination of parameters to use. In fact, this combination could be a solution for the lack of sensitivity of such a device, given the significantly higher headspace concentrations in indole and skatole.

In the case of sensory evaluation, using reduced pressure (to generate the headspace VOCs prior to presentation to the assessor) and, hence, increasing the extraction of several free fatty acids in the headspace should not negatively impact the scores attributed, as these molecules have high sensory thresholds and therefore have a low contribution to the generated odor. In fact, decanoic acid and octadecanoic acid have high flavor detection thresholds (200 mg kg⁻¹ and 10,000 mg kg⁻¹ in oil, respectively [48]). This atmosphere change therefore also seems more adapted in this case than using nitrogen. Indeed, pyrroles produced in the nitrogen environment are often attributed with caramel, sweet, corn and bread flavors. Similarly, pyridines are known to confer green, sweet and nutty odors [49]. Therefore, although a nitrogen environment could be beneficial to reduce oxidation products and decrease potential saturation of the nose during sensory evaluation, it would, nonetheless, drastically change the sensory attributes perceived and the resulting attributed scores.

Lastly, although both the nitrogen and reduced pressure atmospheres allow us to reduce the abundance of lipid oxidation-derived products, it is important to keep in mind that sensory attributes of several of these molecules give the typical “fatty” and “fried” odor present when cooking meat. Therefore, even though they are not directly related to boar taint compounds, they constitute the odor perceived by consumers when cooking pork meat (e.g., heptanal and octanal have various sensory attributes depending on their concentrations, but amongst these is found the “fat” sensory attribute [50]). Suppressing these molecules is therefore not necessarily desired for actual at-line sensory analysis.

However, using a reduced pressure atmosphere could be interesting for an additional step in the protocols used to train assessors prior to sensory evaluation. In fact, the training first involves practicing the detection of pure chemical substances, such as skatole and androstenone, and only later does training on real heated fat samples take place [51]. Adding an in-between step in which fat samples would be heated under reduced pressure atmosphere conditions prior to assessment could be interesting. This step would allow the assessor to recognize the odor of boar taint compounds without background odor resulting from fat heating. Only once the assessor has been trained in understanding and recognizing the natural variations in boar taint would he be confronted with the real odor composed of boar taint compounds and artifacts of lipid oxidation.

5. Conclusions

In this study, VOC profiles obtained following the heating of pig backfat under 9 different combinations of temperature and atmosphere ($T = 150, 300$ and $450\text{ }^{\circ}\text{C}$, ATM = air, nitrogen and reduced pressure atmosphere) were compared. Through the PCA, a strong effect of the sampling atmosphere was pointed out. The VOC profiles obtained under the air and nitrogen atmospheres presented a large diversity of molecules compared to those sampled under reduced pressure atmosphere conditions. This diversity is due, in the first case, to the generation of several compounds in the presence of oxygen, such as aldehydes, which are typically produced through the oxidation of lipids. In the second case, a large amount of nitrogenated compounds are produced, which are typically generated following the pyrolysis of amino acids. In reduced pressure atmosphere environments, a net increase in the headspace of several molecules intrinsic to backfat was observed. These include semi-volatiles, which see their extraction rate increase in such conditions. When looking at the response curves of boar taint-specific compounds, several behaviors are observed. However, most of the analyzed compounds see a maximum extraction yield with a heating temperature of $450\text{ }^{\circ}\text{C}$ under a reduced pressure atmosphere.

Taking into account both the general analysis of the VOC profiles and the analysis of the boar taint compounds, it seems that the reduced pressure atmosphere sampling at $450\text{ }^{\circ}\text{C}$ is the best combination of parameters to extract maximum boar taint compounds when simultaneously reducing the extraction and production of heating artifacts. This combination seems interesting to use for all VOC-based methods. Obtaining higher concentrations of boar taint compounds and lower diversity of other compounds is desired to better detect boar taint, regardless of the method used.

Author Contributions: Conceptualization, C.B., A.M. and M.-L.F.; methodology, C.B., A.M. and M.-L.F.; software, C.B., A.M., Y.B. and M.-L.F.; validation, C.B., A.M., Y.B. and M.-L.F.; formal analysis, C.B., A.M., Y.B. and M.-L.F.; investigation, C.B. and A.M.; resources, C.B., A.M. and M.-L.F.; data curation, C.B., A.M. and Y.B.; writing—original draft preparation, C.B. and A.M.; writing—review and editing, C.B., A.M., Y.B. and M.-L.F.; visualization, C.B. and A.M.; supervision, M.-L.F.; project administration, M.-L.F.; funding acquisition, M.-L.F. All authors have read and agreed to the published version of the manuscript.

Funding: This research was funded by the European Regional Development Fund (ERDF) and the Walloon Region of Belgium, through the Interreg V France-Wallonie-Vlaanderen program, under the PATHACOV project (No. 1.1.297); and the Micro+ project co-funded by the ERDF and Wallonia, Belgium (No. 675781-642409). This article was written within the framework of the AGROSENSOR project, which is part of the “Pole de compétitivité WAGRALIM,” and was financially supported by the “Service public de Wallonie” (SPW).

Institutional Review Board Statement: Not applicable.

Informed Consent Statement: Not applicable.

Data Availability Statement: Data will be available upon request from the corresponding author.

Acknowledgments: The authors would like to thank Andrew Zicler for his great help in the conception and fabrication of the 3D-printed enclosure. Franck Michels, Thomas Bertrand and Danny

Trisman are also thanked for their technical contributions to this work. All figures were created with biorender.com.

Conflicts of Interest: The authors declare no conflict of interest.

Appendix A

Table A1. Fatty acid composition (% , mean \pm stdev) for sows ($n = 5$) and boars ($n = 11$) used in the experiment.

Fatty Acid	Boar	Sow
C6:0	0.01 \pm 0.01	0.01 \pm 0.01
C10:0	0.01 \pm 0.01	0.00 \pm 0.00
C12:0	0.04 \pm 0.02	0.03 \pm 0.02
C14:0	1.27 \pm 0.04	1.14 \pm 0.02
C15:0	0.02 \pm 0.01	0.04 \pm 0.04
C16:0	22.12 \pm 0.21	22.08 \pm 0.20
C17:0	0.38 \pm 0.02	0.23 \pm 0.01
C18:0	13.21 \pm 0.35	13.25 \pm 0.12
C20:0	0.66 \pm 0.02	0.21 \pm 0.11
C21:0	0.03 \pm 0.02	0.07 \pm 0.01
C22:0	0.00 \pm 0.00	0.02 \pm 0.01
C23:0	0.00 \pm 0.01	0.01 \pm 0.01
Σ SFA	37.75	37.09
C16:1	2.05 \pm 0.07	2.07 \pm 0.03
C17:1	0.22 \pm 0.03	0.17 \pm 0.00
C18:1n-9 cis	34.06 \pm 0.47	35.08 \pm 0.08
C18:1n-9 trans	2.13 \pm 0.16	2.11 \pm 0.08
C20:1n-9	0.10 \pm 0.06	0.20 \pm 0.1
C24:1n-9	0.03 \pm 0.03	0.15 \pm 0.02
Σ MUFA	38.59	39.78
C18:2	19.10 \pm 0.42	16.90 \pm 0.12
C18-3n-3	3.26 \pm 0.35	4.89 \pm 0.08
C20:2	0.68 \pm 0.02	0.62 \pm 0.00
C20:3n-6	0.45 \pm 0.01	0.57 \pm 0.00
C20:4n-6	0.17 \pm 0.04	0.15 \pm 0.00
Σ PUFA	23.66	23.13
Total	100.00	100.00

Appendix B

Table A2. Quantification of skatole and androstenone in boar fat determined by HPLC-FD.

Sample Number	Fat Content (ng g ⁻¹ of Fat)	
	Skatole	Androstenone
1	23.5 \pm 4.9	3751.9 \pm 316.1
2	39.6 \pm 3.1	3506.2 \pm 412.4
3	422.7 \pm 186.2	743.1 \pm 309.9
4	257.1 \pm 20.6	3577.0 \pm 116.1
5	214.2 \pm 36.6	398.8 \pm 8.0
6	99.6 \pm 11.0	2169.9 \pm 310.5
7	345.1 \pm 78.1	353.9 \pm 190.8
8	213.0 \pm 27.9	3801.8 \pm 234.5
9	27.4 \pm 2.5	4689.9 \pm 86.9
10	42.1 \pm 15.6	2005.0 \pm 417.4
11	19.6 \pm 1.0	3150.1 \pm 947.5

Appendix C

Table A3. Match factor (MF), CAS number, calculated and literature retention index (calc. and lit. RI) and relative abundance (%; mean \pm standard deviation) for each temperature–atmosphere combination: A150 (150 °C–air); N150 (150 °C–nitrogen); RP150 (150 °C–reduced pressure); A300 (300 °C–air); N300 (300 °C–nitrogen); RP150 (300 °C–reduced pressure); A450 (450 °C–air); N150 (450 °C–nitrogen); RP150 (450 °C–reduced pressure). Undetected compounds are annotated as “n.d.”.

	MF	CAS	Calc. RI	Lit. RI	A150	N150	RP150	A300	N300	RP300	A450	N450	RP450
Alcohols													
Pentan-1-ol	93	71-41-0	768	768	0.08 \pm 0.23	n.d.	n.d.	0.48 \pm 0.22	n.d.	n.d.	0.05 \pm 0.15	n.d.	n.d.
Hexan-1-ol	91	111-27-3	865	865	n.d.	n.d.	n.d.	0.08 \pm 0.11	n.d.	n.d.	0.04 \pm 0.07	0.02 \pm 0.09	n.d.
Heptan-1-ol	93	111-70-6	970	970	0.15 \pm 0.33	n.d.	n.d.	0.69 \pm 0.39	n.d.	n.d.	0.03 \pm 0.12	n.d.	n.d.
Oct-1-en-3-ol	93	3391-86-4	980	980	0.27 \pm 0.59	n.d.	n.d.	1.12 \pm 0.49	n.d.	n.d.	0.27 \pm 0.30	0.03 \pm 0.10	n.d.
Phenol	90	108-95-2	988	989	n.d.	n.d.	n.d.	n.d.	n.d.	n.d.	0.05 \pm 0.15	0.61 \pm 0.84	0.86 \pm 1.21
2,4-Dimethylcyclohexanol	86	69542-91-2	1034	1032	0.01 \pm 0.04	n.d.	n.d.	0.14 \pm 0.09	n.d.	n.d.	n.d.	n.d.	n.d.
Octan-1-ol	92	111-87-5	1073	1073	0.20 \pm 0.56	n.d.	n.d.	1.04 \pm 0.55	n.d.	n.d.	0.22 \pm 0.34	n.d.	n.d.
4-Methylphenol	87	106-44-5	1082	1082	n.d.	n.d.	n.d.	n.d.	n.d.	0.03 \pm 0.12	0.03 \pm 0.15	0.40 \pm 0.85	1.37 \pm 1.95
Nonan-1-ol	89	143-08-8	1173	1173	n.d.	n.d.	n.d.	0.06 \pm 0.10	n.d.	n.d.	n.d.	n.d.	n.d.
(Z)-Tetradec-9-en-1-ol	89	35153-15-2	1670	1667	n.d.	n.d.	n.d.	0.01 \pm 0.03	n.d.	n.d.	0.03 \pm 0.06	0.02 \pm 0.07	0.02 \pm 0.10
<i>Total alcohols</i>					0.71	n.d.	n.d.	3.62	n.d.	0.03	0.72	1.08	2.25
Aldehydes													
Unknown aldehyde			682		0.01 \pm 0.04	n.d.	n.d.	0.10 \pm 0.09	n.d.	n.d.	n.d.	0.02 \pm 0.07	n.d.
2-Methylbutanal	85	96-17-3	706	689	n.d.	n.d.	n.d.	0.00 \pm 0.01	0.13 \pm 0.30	0.00 \pm 0.01	0.01 \pm 0.03	0.18 \pm 0.13	1.39 \pm 5.85
Pentanal	91	110-62-3	712	711	0.69 \pm 1.50	n.d.	n.d.	1.47 \pm 0.73	0.15 \pm 0.31	n.d.	0.67 \pm 0.42	0.10 \pm 0.13	0.97 \pm 4.12
(E)-Pent-2-enal	92	1576-87-0	758	758	0.01 \pm 0.04	n.d.	n.d.	0.03 \pm 0.06	n.d.	n.d.	n.d.	n.d.	n.d.
Hexanal	91	66-25-1	797	797	12.12 \pm 21.16	11.85 \pm 29.70	5.56 \pm 10.09	2.38 \pm 1.27	3.58 \pm 7.02	0.14 \pm 0.56	1.92 \pm 0.68	0.08 \pm 0.32	n.d.
(E)-Hex-2-enal	95	6728-26-3	847	847	0.01 \pm 0.04	n.d.	n.d.	0.13 \pm 0.07	n.d.	n.d.	0.26 \pm 0.19	0.01 \pm 0.05	n.d.
Heptanal	95	111-71-7	900	900	0.84 \pm 1.66	n.d.	0.28 \pm 1.03	2.88 \pm 0.71	0.22 \pm 0.45	n.d.	2.78 \pm 1.01	0.22 \pm 0.81	n.d.
(E)-Hept-2-enal	92	18829-55-5	952	952	1.88 \pm 3.55	n.d.	n.d.	7.26 \pm 2.04	0.01 \pm 0.06	n.d.	3.41 \pm 1.41	0.22 \pm 0.91	n.d.
Benzaldehyde	93	100-52-7	959	959	0.00 \pm 0.01	n.d.	n.d.	0.14 \pm 0.06	0.18 \pm 0.38	0.00 \pm 0.01	0.70 \pm 0.65	0.44 \pm 0.31	0.01 \pm 0.04
(2E,4E)-Hepta-2,4-dienal	92	05-03-13	1003	1003	1.06 \pm 2.63	n.d.	n.d.	5.21 \pm 2.89	0.04 \pm 0.18	n.d.	1.45 \pm 1.46	0.10 \pm 0.30	n.d.
Octanal	95	124-13-0	1010	1010	1.55 \pm 2.94	n.d.	0.29 \pm 1.05	4.29 \pm 0.84	1.07 \pm 1.57	n.d.	3.56 \pm 1.05	0.42 \pm 1.22	n.d.
5-Ethylcyclopentene-1-carbaldehyde	84	36431-60-4	1031	1035	0.03 \pm 0.10	n.d.	n.d.	0.03 \pm 0.03	n.d.	n.d.	0.00 \pm 0.01	n.d.	n.d.
(E)-Oct-2-enal	95	2548-87-0	1059	1059	0.91 \pm 1.64	n.d.	0.17 \pm 0.60	3.06 \pm 0.49	0.13 \pm 0.32	n.d.	2.53 \pm 0.94	0.26 \pm 0.78	n.d.
2-Phenylacetaldehyde	88	122-78-1	1063	1061	n.d.	n.d.	n.d.	0.03 \pm 0.04	0.38 \pm 0.42	0.01 \pm 0.03	0.01 \pm 0.02	0.12 \pm 0.29	n.d.
(E)-Non-4-enal	84	2277-16-9	1094	1096	n.d.	n.d.	n.d.	0.07 \pm 0.07	n.d.	n.d.	n.d.	n.d.	n.d.
Nonanal	96	124-19-6	1111	1111	23.33 \pm 21.82	27.08 \pm 34.28	13.65 \pm 27.22	16.17 \pm 3.75	11.84 \pm 10.97	0.21 \pm 0.48	7.88 \pm 3.58	1.41 \pm 2.54	n.d.

Table A3. Cont.

	MF	CAS	Calc. RI	Lit. RI	A150	N150	RP150	A300	N300	RP300	A450	N450	RP450
(Z)-Non-2-enal	88	60784-31-8	1148	1148	0.04 ± 0.15	n.d.	n.d.	0.26 ± 0.13	n.d.	n.d.	0.20 ± 0.27	n.d.	n.d.
(E)-Non-2-enal	92	18829-56-6	1161	1161	0.42 ± 0.91	n.d.	n.d.	2.14 ± 0.66	0.36 ± 0.68	n.d.	1.82 ± 0.87	0.23 ± 0.65	n.d.
(Z)-Dec-7-enal	87	21661-97-2	1189	1179	n.d.	n.d.	n.d.	0.31 ± 0.21	n.d.	n.d.	0.03 ± 0.14	n.d.	n.d.
Decanal	97	112-31-2	1211	1211	1.73 ± 4.28	0.25 ± 0.90	n.d.	4.25 ± 1.03	1.79 ± 1.61	n.d.	5.91 ± 2.57	2.16 ± 0.79	0.12 ± 0.00
(2E,4E)-Nona-2,4-dienal	86	5910-87-2	1213	1213	0.02 ± 0.08	n.d.	n.d.	0.13 ± 0.09	n.d.	n.d.	0.03 ± 0.08	n.d.	n.d.
(Z)-Dec-2-enal	88	2497-25-8	1250	1250	0.09 ± 0.37	n.d.	n.d.	1.15 ± 0.37	n.d.	n.d.	0.80 ± 0.47	0.03 ± 0.14	n.d.
(E)-Dec-2-enal	92	3913-81-3	1271	1273	3.71 ± 5.76	1.82 ± 4.59	3.92 ± 9.46	10.17 ± 1.28	11.13 ± 13.13	0.42 ± 1.05	5.39 ± 2.33	0.89 ± 2.03	0.07 ± 0.29
(2E,4E)-Deca-2,4-dienal	91	25152-84-5	1290	1293	3.22 ± 6.92	n.d.	0.53 ± 1.89	10.19 ± 3.77	9.28 ± 16.27	0.81 ± 2.27	3.81 ± 1.93	3.26 ± 3.71	0.39 ± 0.92
Undecanal	98	112-44-7	1309	1309	0.25 ± 0.57	0.18 ± 0.63	n.d.	1.87 ± 0.86	0.47 ± 1.11	n.d.	1.51 ± 1.04	0.09 ± 0.36	n.d.
(E)-Undec-2-enal	94	2463-77-6	1388	1386	2.62 ± 4.80	1.82 ± 4.53	7.57 ± 14.72	7.35 ± 1.59	5.01 ± 6.00	1.70 ± 3.37	4.17 ± 1.55	1.16 ± 1.08	0.17 ± 0.40
Dodecanal	97	112-54-9	1410	1410	0.18 ± 0.41	n.d.	n.d.	1.10 ± 0.50	0.53 ± 1.23	n.d.	0.98 ± 0.50	0.02 ± 0.08	n.d.
Tridecanal	97	10486-19-8	1511	1511	0.02 ± 0.08	n.d.	n.d.	0.36 ± 0.23	n.d.	n.d.	0.26 ± 0.22	n.d.	n.d.
Tetradecanal	93	124-25-4	1613	1613	0.01 ± 0.02	n.d.	n.d.	0.10 ± 0.10	n.d.	0.03 ± 0.13	0.04 ± 0.08	n.d.	n.d.
Pentadecanal	89	09-11-65	1715	1715	n.d.	0.30 ± 1.07	n.d.	0.06 ± 0.09	n.d.	0.09 ± 0.37	0.03 ± 0.08	n.d.	n.d.
<i>Total aldehydes</i>					54.75	43.30	31.97	82.69	46.30	3.41	50.16	11.42	3.12
Alkanes													
Unknown alkane A			722		0.04 ± 0.18	n.d.	0.04 ± 0.14	0.03 ± 0.14	0.24 ± 0.60	n.d.	0.25 ± 0.45	0.15 ± 0.22	0.01 ± 0.03
1-Ethyl-2-methylcyclopentane	91	930-89-2	787	783	0.02 ± 0.08	n.d.	n.d.	0.01 ± 0.04	n.d.	n.d.	0.29 ± 0.71	n.d.	n.d.
Octane	90	111-65-9	795	800	1.10 ± 2.54	1.26 ± 4.56	n.d.	0.10 ± 0.43	5.50 ± 22.89	n.d.	0.16 ± 0.19	0.54 ± 0.45	3.21 ± 13.60
Nonane	94	111-84-2	897	900	n.d.	n.d.	n.d.	0.31 ± 0.24	n.d.	n.d.	0.66 ± 0.52	0.36 ± 0.41	0.01 ± 0.03
Propylcyclohexane	85	1678-92-8	926	927	n.d.	n.d.	n.d.	0.03 ± 0.03	n.d.	n.d.	n.d.	n.d.	n.d.
Butylcyclopentane	91	2040-95-1	930	930	0.01 ± 0.04	n.d.	n.d.	0.13 ± 0.08	n.d.	n.d.	0.11 ± 0.11	0.01 ± 0.05	n.d.
Decane	92	124-18-5	999	1000	0.03 ± 0.10	n.d.	n.d.	0.69 ± 0.42	0.02 ± 0.08	n.d.	0.91 ± 0.82	0.53 ± 0.53	0.01 ± 0.06
Methylcyclooctane	91	1502-38-1	1094	1020	n.d.	n.d.	n.d.	n.d.	n.d.	n.d.	1.88 ± 2.06	0.15 ± 0.62	n.d.
Undecane	95	1120-21-4	1110	1100	0.05 ± 0.15	n.d.	n.d.	1.16 ± 0.66	0.10 ± 0.32	n.d.	2.20 ± 0.54	1.07 ± 0.83	0.04 ± 0.14
Dodecane	85	112-40-3	1199	1200	0.02 ± 0.08	0.08 ± 0.28	n.d.	0.02 ± 0.06	0.12 ± 0.41	n.d.	n.d.	n.d.	0.10 ± 0.23
Tridecane	95	629-50-5	1299	1300	0.07 ± 0.19	0.30 ± 0.75	0.27 ± 0.96	1.10 ± 0.62	1.28 ± 1.67	n.d.	2.38 ± 0.67	2.25 ± 1.41	0.41 ± 0.61
Tetradecane	95	629-59-4	1400	1400	0.02 ± 0.07	0.35 ± 0.92	n.d.	0.71 ± 0.38	0.48 ± 0.88	0.04 ± 0.18	1.41 ± 0.73	1.63 ± 1.29	1.00 ± 0.82
Nonylcyclopentane	92	2882-98-6	1448	1451	0.01 ± 0.02	n.d.	n.d.	0.13 ± 0.08	0.03 ± 0.14	n.d.	0.33 ± 0.28	0.17 ± 0.22	0.01 ± 0.06
Pentadecane	96	629-62-9	1497	1500	0.68 ± 1.83	2.34 ± 3.83	4.84 ± 7.01	0.70 ± 0.35	2.02 ± 2.55	1.29 ± 1.98	2.24 ± 1.29	3.38 ± 2.16	4.09 ± 2.31
Nonylcyclohexane	88	05-02-83	1551	1551	n.d.	n.d.	0.02 ± 0.09	0.04 ± 0.03	0.02 ± 0.11	0.07 ± 0.22	0.18 ± 0.17	0.13 ± 0.17	0.15 ± 0.23
Hexadecane	90	544-76-3	1602	1600	n.d.	n.d.	0.17 ± 0.61	0.11 ± 0.08	n.d.	0.09 ± 0.32	0.02 ± 0.06	0.20 ± 0.32	0.64 ± 0.81
Heptadecane	91	629-78-7	1699	1700	0.09 ± 0.33	0.51 ± 1.32	1.04 ± 1.85	0.01 ± 0.02	0.15 ± 0.64	0.49 ± 1.38	0.37 ± 0.38	0.31 ± 0.59	2.35 ± 2.64
<i>Total alkanes</i>					2.14	4.84	6.38	5.28	9.96	1.98	13.39	10.88	12.03
Alkenes													
3-Methylcyclopentene	87	1120-62-3	695	671	n.d.	n.d.	n.d.	n.d.	n.d.	n.d.	0.07 ± 0.13	0.00 ± 0.01	n.d.
Cyclohexa-1,4-diene	87	628-41-1	712	707	n.d.	n.d.	n.d.	0.01 ± 0.01	n.d.	n.d.	0.03 ± 0.03	0.00 ± 0.01	n.d.
Cyclohexene	91	110-83-8	713	707	n.d.	n.d.	n.d.	n.d.	n.d.	n.d.	0.04 ± 0.06	0.00 ± 0.01	n.d.
Hept-1-ene	94	592-76-7	717	707	n.d.	n.d.	n.d.	0.03 ± 0.05	n.d.	n.d.	0.64 ± 0.50	0.09 ± 0.13	n.d.
Hept-2-ene	84	592-77-8	726	702	n.d.	n.d.	n.d.	n.d.	n.d.	n.d.	0.03 ± 0.05	0.00 ± 0.01	n.d.

Table A3. Cont.

	MF	CAS	Calc. RI	Lit. RI	A150	N150	RP150	A300	N300	RP300	A450	N450	RP450
3-Methylcyclohexene	91	591-48-0	745	745	n.d.	n.d.	n.d.	n.d.	0.01 ± 0.06	n.d.	0.09 ± 0.06	0.04 ± 0.04	n.d.
3-Methylcyclohexene	86	591-48-0	747	745	n.d.	n.d.	n.d.	n.d.	n.d.	n.d.	0.03 ± 0.04	n.d.	n.d.
1-Methylcyclohexa-1,4-diene	88	4313-57-9	778	780	n.d.	n.d.	n.d.	n.d.	n.d.	n.d.	0.04 ± 0.05	n.d.	n.d.
Oct-1-ene	93	111-66-0	787	788	0.00 ± 0.02	n.d.	n.d.	0.06 ± 0.08	n.d.	n.d.	0.71 ± 0.70	0.17 ± 0.25	n.d.
(Z)-Oct-2-ene	87	08-04-42	803	803	n.d.	n.d.	n.d.	0.02 ± 0.04	n.d.	n.d.	0.23 ± 0.22	0.09 ± 0.19	n.d.
(3E)-Octa-1,3-diene	90	1002-33-1	819	825	n.d.	n.d.	n.d.	n.d.	n.d.	n.d.	0.31 ± 0.27	0.02 ± 0.05	n.d.
5-Ethylcyclohexa-1,3-diene	84	40085-08-3	832	844	n.d.	n.d.	n.d.	n.d.	n.d.	n.d.	0.02 ± 0.03	n.d.	n.d.
1-Propylcyclopentene	87	3074-61-1	840	840	n.d.	n.d.	n.d.	n.d.	n.d.	n.d.	0.03 ± 0.05	n.d.	n.d.
(3E,5Z)-Octa-1,3,5-triene	86	33580-05-1	875	880	n.d.	n.d.	n.d.	0.01 ± 0.01	n.d.	n.d.	0.09 ± 0.13	0.05 ± 0.14	n.d.
Nona-1,8-diene	86	4900-30-5	878	880	n.d.	n.d.	n.d.	n.d.	n.d.	n.d.	0.04 ± 0.10	n.d.	n.d.
Non-1-ene	88	124-11-8	888	888	0.06 ± 0.23	n.d.	n.d.	n.d.	n.d.	n.d.	1.83 ± 1.10	0.46 ± 0.65	n.d.
(Z)-Non-2-ene	85	6434-77-1	906	903	n.d.	n.d.	n.d.	n.d.	n.d.	n.d.	0.10 ± 0.20	0.01 ± 0.02	n.d.
3-Butylcyclopentene	86	22531-00-6	919	916	n.d.	n.d.	n.d.	0.00 ± 0.01	n.d.	n.d.	0.14 ± 0.15	0.01 ± 0.04	n.d.
(3E)-Nona-1,3-diene	86	56700-77-7	923	924	n.d.	n.d.	n.d.	n.d.	n.d.	n.d.	0.46 ± 0.54	0.02 ± 0.09	n.d.
1-Butylcyclopentene	92	2423-01-0	945	940	n.d.	n.d.	n.d.	0.01 ± 0.06	n.d.	n.d.	0.71 ± 0.60	0.05 ± 0.22	n.d.
Dec-1-ene	92	872-05-9	991	993	0.15 ± 0.61	n.d.	n.d.	n.d.	n.d.	n.d.	1.31 ± 1.19	0.66 ± 0.60	n.d.
(Z)-Dec-5-ene	90	7433-78-5	1004	993	n.d.	0.04 ± 0.08	n.d.						
Undec-1-ene	95	821-95-4	1091	1092	0.17 ± 0.66	n.d.	n.d.	0.03 ± 0.11	0.03 ± 0.12	n.d.	0.84 ± 1.46	1.48 ± 1.07	0.06 ± 0.27
(E)-Undec-2-ene	92	693-61-8	1104	1104	n.d.	n.d.	n.d.	0.05 ± 0.07	0.02 ± 0.08	n.d.	0.86 ± 0.61	2.49 ± 1.99	0.01 ± 0.05
1-Hexylcyclopentene	86	4291-99-0	1125	1129	0.02 ± 0.07	n.d.	n.d.	0.02 ± 0.09	n.d.	n.d.	1.35 ± 1.58	1.58 ± 1.73	0.06 ± 0.18
(3Z,5E)-Undeca-1,3,5-triene	86	19883-27-3	1166	1174	0.01 ± 0.03	n.d.	n.d.	0.04 ± 0.04	0.03 ± 0.13	n.d.	1.09 ± 0.56	1.36 ± 1.58	0.06 ± 0.13
Dodec-1-ene	92	25378-22-7	1193	1193	0.18 ± 0.64	0.24 ± 0.88	n.d.	0.05 ± 0.13	0.26 ± 0.70	n.d.	2.12 ± 1.89	1.58 ± 1.55	0.26 ± 0.58
Tridec-1-ene	94	2437-56-1	1292	1292	0.02 ± 0.08	0.23 ± 0.84	n.d.	0.03 ± 0.08	0.15 ± 0.40	n.d.	2.66 ± 1.34	1.48 ± 1.43	0.49 ± 0.85
(E)-Tetradec-7-ene	88	10374-74-0	1388	1390	n.d.	n.d.	n.d.	0.04 ± 0.05	n.d.	n.d.	0.18 ± 0.13	0.07 ± 0.15	n.d.
Tetradec-1-ene	96	1120-36-1	1392	1392	0.46 ± 1.71	0.57 ± 2.05	0.55 ± 1.98	0.16 ± 0.22	0.42 ± 0.93	0.03 ± 0.11	0.65 ± 1.11	2.22 ± 1.75	1.31 ± 1.41
Pentadec-1-ene	90	13360-61-7	1488	1488	0.02 ± 0.06	n.d.	0.20 ± 0.71	0.19 ± 0.18	0.28 ± 0.78	0.05 ± 0.15	0.90 ± 0.82	1.33 ± 1.78	1.79 ± 2.02
(Z)-Hexadec-7-ene	90	35507-09-6	1580	1568	n.d.	n.d.	0.05 ± 0.18	0.09 ± 0.08	n.d.	n.d.	0.09 ± 0.23	0.10 ± 0.27	0.09 ± 0.39
Hexadec-1-ene	94	629-73-2	1591	1591	n.d.	n.d.	n.d.	0.03 ± 0.08	n.d.	0.09 ± 0.22	0.40 ± 0.32	0.23 ± 0.36	0.84 ± 0.94
(E)-Heptadec-3-ene	91	68155-00-0	1677	1684	n.d.	n.d.	1.30 ± 2.29	0.14 ± 0.11	0.22 ± 0.64	0.69 ± 1.35	0.66 ± 0.64	0.84 ± 0.83	3.82 ± 1.78
Total alkenes					1.09	1.04	2.10	1.01	1.42	0.86	18.75	16.47	8.79
Amides													
Pyridine-2-carboxamide	87	1452-77-3	1265	1268	n.d.	n.d.	n.d.	n.d.	n.d.	0.10 ± 0.25	n.d.	n.d.	0.80 ± 1.12
Hexadecanamide	87	629-54-9	2190	2186	0.66 ± 2.66	0.26 ± 0.93	n.d.	0.03 ± 0.13	0.02 ± 0.09	0.14 ± 0.39	0.06 ± 0.18	0.22 ± 0.33	1.59 ± 1.20
(Z)-Octadec-9-enamide	85	301-02-0	2369	2375	n.d.	n.d.	n.d.	0.03 ± 0.12	n.d.	n.d.	0.04 ± 0.19	0.15 ± 0.35	1.00 ± 1.38
Octadecanamide	85	124-26-5	2396	2398	n.d.	n.d.	n.d.	n.d.	n.d.	n.d.	0.02 ± 0.09	0.02 ± 0.08	0.41 ± 0.69
Total amides					0.66	0.26	n.d.	0.06	0.02	0.24	0.12	0.39	3.80
Amines													
2-(Dimethylamino)ethanol	89	108-01-0	739	711	n.d.	n.d.	n.d.	0.01 ± 0.02	0.07 ± 0.22	0.06 ± 0.20	0.02 ± 0.06	0.32 ± 0.44	0.75 ± 1.33
Pyridin-2-amine	90	504-29-0	1009	1002	n.d.	0.15 ± 0.62	1.17 ± 1.58						
4-Methylaniline	94	106-49-0	1027	1068	n.d.	n.d.	n.d.	0.01 ± 0.01	0.10 ± 0.27	n.d.	0.04 ± 0.08	0.18 ± 0.30	0.02 ± 0.04

Table A3. Cont.

	MF	CAS	Calc. RI	Lit. RI	A150	N150	RP150	A300	N300	RP300	A450	N450	RP450
2,4,6-Trimethylaniline	85	88-05-1	1256	1261	n.d.	n.d.	n.d.	n.d.	n.d.	n.d.	n.d.	0.28 ± 0.43	0.00 ± 0.02
<i>Total amines</i>					n.d.	n.d.	n.d.	0.02	0.17	0.06	0.06	0.93	1.94
Benzene derivatives													
Toluene	93	108-88-3	799	796	n.d.	n.d.	n.d.	0.02 ± 0.02	0.16 ± 0.24	n.d.	0.51 ± 0.44	2.29 ± 1.60	0.06 ± 0.10
Ethylbenzene	90	100-41-4	855	855	n.d.	n.d.	n.d.	n.d.	n.d.	n.d.	0.19 ± 0.12	0.67 ± 0.48	n.d.
1,3-Xylene	84	108-38-3	864	864	n.d.	n.d.	n.d.	n.d.	n.d.	n.d.	0.01 ± 0.03	0.03 ± 0.05	n.d.
Styrene	93	100-42-5	887	887	n.d.	n.d.	n.d.	n.d.	n.d.	n.d.	0.12 ± 0.11	0.42 ± 0.30	n.d.
Propylbenzene	93	103-65-1	951	950	n.d.	n.d.	n.d.	0.00 ± 0.01	0.01 ± 0.03	n.d.	0.19 ± 0.09	0.30 ± 0.13	0.00 ± 0.01
2,3-Dihydro-1H-indene	85	496-11-7	1025	1027	n.d.	n.d.	n.d.	n.d.	n.d.	n.d.	0.06 ± 0.08	0.26 ± 0.19	0.00 ± 0.01
1-Ethynyl-4-methylbenzene	86	766-97-2	1043	1004	n.d.	n.d.	n.d.	n.d.	n.d.	n.d.	0.03 ± 0.04	0.04 ± 0.05	0.00 ± 0.02
1H-indene	88	95-13-6	1043	1042	n.d.	n.d.	n.d.	n.d.	n.d.	n.d.	0.02 ± 0.07	0.03 ± 0.07	0.03 ± 0.06
Butylbenzene	89	104-51-8	1076	1078	n.d.	n.d.	n.d.	0.05 ± 0.06	0.13 ± 0.22	0.00 ± 0.01	0.45 ± 0.18	0.66 ± 0.29	0.02 ± 0.04
Unknown benzene derivative			1126		n.d.	n.d.	n.d.	n.d.	n.d.	n.d.	0.07 ± 0.10	0.12 ± 0.19	n.d.
1,2-Dihydronaphthalene	84	447-53-0	1151	1149	n.d.	n.d.	n.d.	n.d.	n.d.	n.d.	0.02 ± 0.07	0.04 ± 0.07	n.d.
Pentylbenzene	89	538-68-1	1158	1158	n.d.	n.d.	n.d.	0.06 ± 0.10	0.10 ± 0.36	n.d.	0.76 ± 0.39	0.82 ± 0.91	0.03 ± 0.08
1-Butyl-4-methylbenzene	87	2719-52-0	1168	1127	n.d.	n.d.	n.d.	n.d.	n.d.	n.d.	0.07 ± 0.08	0.17 ± 0.24	0.01 ± 0.03
Naphthalene	86	91-20-3	1184	1183	n.d.	n.d.	n.d.	n.d.	n.d.	n.d.	0.08 ± 0.13	0.15 ± 0.21	0.02 ± 0.06
Hexylbenzene	84	1077-16-3	1261	1260	n.d.	n.d.	n.d.	0.01 ± 0.02	n.d.	n.d.	0.19 ± 0.22	0.34 ± 0.58	0.01 ± 0.04
Heptylbenzene	84	1078-71-3	1364	1362	n.d.	n.d.	n.d.	0.00 ± 0.01	0.04 ± 0.16	n.d.	0.10 ± 0.16	0.35 ± 0.36	0.05 ± 0.12
2,6-Ditert-butyl-4-methylphenol	87	128-37-0	1527	1524	n.d.	0.06 ± 0.23	15.50 ± 37.50	0.25 ± 0.75	4.18 ± 7.04	0.39 ± 0.79	0.01 ± 0.03	0.12 ± 0.28	0.10 ± 0.35
Dodecan-6-ylbenzene	82	2719-62-2	1733	1727	n.d.	n.d.	8.05 ± 27.64	n.d.	n.d.	0.01 ± 0.02	n.d.	n.d.	n.d.
<i>Total benzene derivatives</i>					n.d.	0.06	23.55	0.39	4.62	0.40	2.89	6.86	0.33
Fatty acids													
Nonanoic acid	86	112-05-0	1280	1280	n.d.	n.d.	n.d.	n.d.	n.d.	0.08 ± 0.19	n.d.	n.d.	0.07 ± 0.28
Methyl hexadecanoate	85	112-39-0	1926	1925	n.d.	n.d.	n.d.	n.d.	n.d.	0.18 ± 0.30	n.d.	n.d.	0.26 ± 0.27
(Z)-Hexadec-11-enoic acid	84	2416-20-8	1947	1953	n.d.	n.d.	n.d.	n.d.	n.d.	1.01 ± 1.64	n.d.	0.07 ± 0.29	0.29 ± 1.24
Hexadecanoic acid	94	57-10-3	1965	1965	8.75 ± 19.22	11.06 ± 15.47	5.75 ± 9.79	1.23 ± 2.86	5.39 ± 8.13	33.46 ± 22.38	3.03 ± 3.55	8.08 ± 5.11	35.52 ± 20.11
2-Dodecanone	88	544-63-8	1397	1401	n.d.	n.d.	n.d.	n.d.	n.d.	1.26 ± 1.79	0.07 ± 0.16	0.58 ± 2.41	1.46 ± 2.37
Methyl (9Z,12Z)-octadeca-9,12-dienoate	89	112-63-0	2095	2095	n.d.	n.d.	0.06 ± 0.20	0.01 ± 0.02	0.14 ± 0.43	1.76 ± 3.10	0.02 ± 0.08	0.07 ± 0.21	0.79 ± 1.27
Methyl (E)-octadec-9-enoate	89	1937-62-8	2101	2100	n.d.	n.d.	0.10 ± 0.36	0.01 ± 0.04	0.28 ± 0.74	3.99 ± 7.56	0.02 ± 0.08	0.09 ± 0.37	1.37 ± 1.87
Methyl octadecanoate	84	112-61-8	2128	2123	n.d.	n.d.	n.d.	n.d.	n.d.	0.04 ± 0.13	n.d.	n.d.	0.08 ± 0.15
(Z)-Octadec-11-enoic acid	91	506-17-2	2134	2141	9.19 ± 25.54	14.34 ± 27.48	8.60 ± 20.99	2.74 ± 5.28	17.00 ± 25.22	34.41 ± 30.77	3.46 ± 6.63	17.74 ± 10.32	6.44 ± 14.98
Octadecanoic acid	90	57-11-4	2161	2161	n.d.	1.70 ± 6.12	1.39 ± 3.40	0.28 ± 0.66	1.28 ± 2.79	7.04 ± 6.86	0.98 ± 1.39	2.36 ± 2.01	8.23 ± 5.29
Decanoic acid	86	334-48-5	3177	1372	n.d.	n.d.	n.d.	n.d.	n.d.	0.18 ± 0.61	n.d.	n.d.	0.12 ± 0.43
<i>Total fatty acids</i>					17.94	27.10	15.90	4.27	24.09	83.41	7.58	28.99	54.63

Table A3. Cont.

	MF	CAS	Calc. RI	Lit. RI	A150	N150	RP150	A300	N300	RP300	A450	N450	RP450
Furans													
2-Methyloxolane	92	96-47-9	708	685	n.d.	n.d.	n.d.	0.00 ± 0.01	n.d.	n.d.	0.43 ± 0.39	0.01 ± 0.06	n.d.
2,5-Dimethyloxolane	94	1003-38-9	729	727	n.d.	n.d.	n.d.	n.d.	n.d.	n.d.	0.13 ± 0.13	0.00 ± 0.02	n.d.
2,5-Diethyloxolane	87	41239-48-9	894	896	n.d.	n.d.	n.d.	n.d.	n.d.	n.d.	0.21 ± 0.25	0.01 ± 0.03	n.d.
2-Pentylfuran	88	3777-69-3	991	990	0.58 ± 1.31	n.d.	n.d.	0.48 ± 0.29	0.45 ± 0.81	n.d.	0.02 ± 0.07	n.d.	n.d.
5-Dodecyloxolan-2-one	86	730-46-1	2106	2106	n.d.	0.23 ± 0.82	1.48 ± 3.15	0.02 ± 0.05	n.d.	0.28 ± 0.56	0.08 ± 0.10	0.01 ± 0.02	0.10 ± 0.31
Total furans					0.58	0.23	1.48	0.50	0.45	0.28	0.87	0.03	0.10
Heterocyclic compounds													
Pyridine	93	110-86-1	750	751	n.d.	n.d.	n.d.	0.04 ± 0.03	2.19 ± 5.87	n.d.	0.20 ± 0.13	0.74 ± 0.39	0.01 ± 0.03
Unknown heterocyclic compound B	86	110-87-2	759	708	n.d.	n.d.	n.d.	0.01 ± 0.03	n.d.	n.d.	0.07 ± 0.08	n.d.	n.d.
1H-Pyrrole	96	109-97-7	760	758	n.d.	n.d.	n.d.	0.03 ± 0.05	0.41 ± 0.94	n.d.	0.79 ± 0.63	3.72 ± 2.05	0.08 ± 0.17
2-Methyl-1H-pyrrole	88	636-41-9	802	799	n.d.	n.d.	n.d.	n.d.	n.d.	n.d.	0.15 ± 0.22	0.94 ± 0.96	0.00 ± 0.02
1-Ethylpyrrole	88	617-92-5	809	810	n.d.	n.d.	n.d.	0.01 ± 0.02	0.14 ± 0.41	n.d.	0.05 ± 0.15	0.54 ± 0.88	n.d.
2-Methylpyridine	88	109-06-8	810	811	n.d.	n.d.	n.d.	0.00 ± 0.01	0.03 ± 0.11	n.d.	0.16 ± 0.15	0.83 ± 0.52	0.01 ± 0.02
3-Methyl-1H-pyrrole	93	616-43-3	844	841	n.d.	n.d.	n.d.	n.d.	n.d.	n.d.	0.03 ± 0.07	0.35 ± 0.37	0.00 ± 0.01
3-Methylpyridine	89	108-99-6	855	856	n.d.	n.d.	n.d.	n.d.	n.d.	n.d.	0.06 ± 0.20	0.27 ± 0.57	0.01 ± 0.05
2,6-Dimethylpyridine	85	108-48-5	879	874	n.d.	n.d.	n.d.	n.d.	n.d.	n.d.	0.01 ± 0.03	0.10 ± 0.07	n.d.
2-Ethylpyridine	90	100-71-0	901	901	n.d.	n.d.	n.d.	0.03 ± 0.02	0.00 ± 0.01	n.d.	0.05 ± 0.07	0.24 ± 0.18	0.00 ± 0.01
2,5-Dimethylpyrazine	87	123-32-0	908	908	n.d.	n.d.	n.d.	n.d.	0.02 ± 0.10	n.d.	0.01 ± 0.02	0.01 ± 0.03	n.d.
2,4-Dimethylpyridine	86	108-47-4	926	925	n.d.	n.d.	n.d.	n.d.	0.05 ± 0.15	n.d.	0.13 ± 0.33	0.90 ± 1.63	0.04 ± 0.11
2,5-Dimethyl-1H-pyrrole	93	625-84-3	936	937	n.d.	n.d.	n.d.	n.d.	n.d.	n.d.	0.02 ± 0.08	0.47 ± 0.30	0.00 ± 0.01
2,5-Dimethylpyridine	90	589-93-5	940	946	n.d.	n.d.	n.d.	n.d.	n.d.	n.d.	0.04 ± 0.11	0.43 ± 0.36	0.01 ± 0.04
3-Ethylpyridine	83	536-78-7	954	955	n.d.	n.d.	n.d.	n.d.	n.d.	n.d.	0.01 ± 0.04	0.08 ± 0.14	n.d.
4-Ethyl-2-methyl-1H-pyrrole	83	5690-96-0	972	951	n.d.	n.d.	n.d.	n.d.	n.d.	n.d.	0.01 ± 0.03	0.23 ± 0.29	n.d.
Pyridin-2-amine	90	504-29-0	1010	1002	n.d.	n.d.	n.d.	n.d.	0.05 ± 0.22	n.d.	0.07 ± 0.14	1.56 ± 0.66	n.d.
2,3,4-Trimethyl-1H-pyrrole	87	3855-78-5	1019	978	n.d.	n.d.	n.d.	n.d.	n.d.	n.d.	0.02 ± 0.11	0.86 ± 0.86	n.d.
2,6-Diethylpyrazine	85	13067-27-1	1079	1080	n.d.	n.d.	n.d.	n.d.	0.19 ± 0.36	n.d.	0.00 ± 0.01	0.05 ± 0.12	n.d.
Unknown heterocyclic compound A	87	496-15-1	1115	1192	n.d.	n.d.	n.d.	0.01 ± 0.02	0.28 ± 0.50	n.d.	0.05 ± 0.12	0.99 ± 0.92	0.02 ± 0.07
2-Isobutyl-4-methylpyridine	87	85665-88-9	1149	1154	n.d.	n.d.	n.d.	n.d.	n.d.	n.d.	0.02 ± 0.08	0.41 ± 0.51	0.05 ± 0.11
2-Pentylpyridine	86	2294-76-0	1197	1202	n.d.	n.d.	n.d.	0.05 ± 0.05	n.d.	n.d.	0.03 ± 0.07	0.23 ± 0.63	n.d.
1-Methylindole	83	603-76-9	1246	1273	n.d.	n.d.	n.d.	n.d.	n.d.	n.d.	n.d.	0.19 ± 0.37	n.d.
1H-Indole	89	120-72-9	1251	1251	n.d.	n.d.	n.d.	0.00 ± 0.02	0.04 ± 0.11	0.17 ± 0.44	0.16 ± 0.24	1.51 ± 1.67	2.04 ± 1.96
3-Methyl-1H-indole	86	83-34-1	1381	1383	n.d.	n.d.	n.d.	n.d.	0.15 ± 0.58	0.02 ± 0.09	n.d.	0.26 ± 0.58	0.60 ± 0.84
Total heterocyclic compounds					n.d.	n.d.	n.d.	0.18	3.55	0.19	2.14	15.91	2.87
Ketones													
Pentan-3-one	82	96-22-0	683	685	6.52 ± 24.95	7.85 ± 27.71	n.d.	0.01 ± 0.02	0.03 ± 0.10	n.d.	0.16 ± 0.23	0.02 ± 0.07	n.d.
Hex-1-en-3-one	91	1629-60-3	775	777	n.d.	n.d.	n.d.	n.d.	n.d.	n.d.	0.14 ± 0.12	0.01 ± 0.02	n.d.
Hexan-3-one	85	589-38-8	784	784	n.d.	n.d.	n.d.	0.03 ± 0.04	n.d.	n.d.	0.01 ± 0.01	0.00 ± 0.01	n.d.

Appendix D

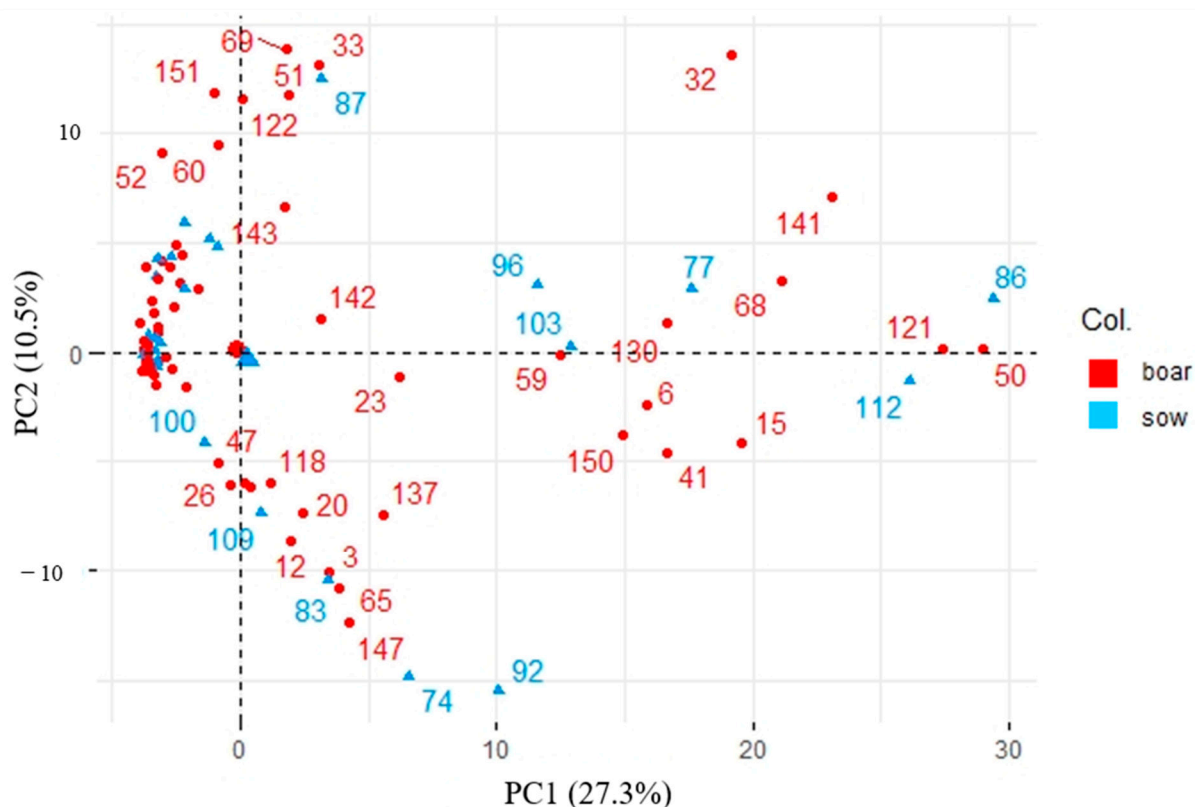


Figure A1. Principal component analysis individual plot comparing backfats based on their VOC profiles. Samples are labeled based on the fat type: red—boar fat, blue—sow fat. Normalized peak areas were used for this PCA.

References

1. Patterson, R.L.S. 5 α -androst-16-ene-3-one:—Compound Responsible for Taint in Boar Fat. *J. Sci. Food Agric.* **1968**, *19*, 31–38. [CrossRef]
2. Vold, E. Fleischproduktionseigenschaften bei Ebern und Kastraten IV: Organoleptische und Gaschromatographische Untersuchungen Wasserdampf flüchtig-Tiger Stoffe Des Rücken-Speckes von Ebern. *Meld. Fra Norges Landbrugshøgskole* **1970**, *49*, 1–25.
3. Brooks, R.I.; Pearson, A.M. Odor Thresholds of the C19- Δ 16-Steroids Responsible for Boar Odor in Pork. *Meat Sci.* **1989**, *24*, 11–19. [CrossRef] [PubMed]
4. Fischer, J.; Gerlach, C.; Meier-Dinkel, L.; Elsinghorst, P.W.; Boeker, P.; Schmarr, H.G.; Wüst, M. 2-Aminoacetophenone—A Hepatic Skatole Metabolite as a Potential Contributor to Boar Taint. *Food Res. Int.* **2014**, *62*, 35–42. [CrossRef]
5. Aluwé, M.; Heyrman, E.; Almeida, J.M.; Babol, J.; Battacone, G.; Čitek, J.; Font-i-Furnols, M.; Getya, A.; Karolyi, D.; Kostyra, E.; et al. Exploratory Survey on European Consumer and Stakeholder Attitudes towards Alternatives for Surgical Castration of Piglets. *Animals* **2020**, *10*, 1758. [CrossRef] [PubMed]
6. European Commission European Declaration on Alternatives to Surgical Castration of Pigs. Available online: https://ec.europa.eu/food/animals/welfare/practice/farm/pigs/castration_alternatives_en (accessed on 15 April 2021).
7. Bonneau, M.; Weiler, U. Pros and Cons of Alternatives to Piglet Castration: Welfare, Boar Taint, and Other Meat Quality Traits. *Animals* **2019**, *9*, 884. [CrossRef]
8. Kress, K.; Weiler, U.; Schmucker, S.; Čandek-Potokar, M.; Vrecl, M.; Fazarinc, G.; Škrlep, M.; Batorek-Lukač, N.; Stefanski, V. Influence of Housing Conditions on Reliability of Immunocastration and Consequences for Growth Performance of Male Pigs. *Animals* **2020**, *10*, 27. [CrossRef]
9. Heyrman, E.; Kowalski, E.; Millet, S.; Tuytens, F.A.M.; Ampe, B.; Janssens, S.; Buys, N.; Wauters, J.; Vanhaecke, L.; Aluwé, M. Monitoring of Behavior, Sex Hormones and Boar Taint Compounds during the Vaccination Program for Immunocastration in Three Sire Lines. *Res. Vet. Sci.* **2019**, *124*, 293–302. [CrossRef]
10. Trautmann, J.; Gertheiss, J.; Wicke, M.; Mörlein, D. How Olfactory Acuity Affects the Sensory Assessment of Boar Fat: A Proposal for Quantification. *Meat Sci.* **2014**, *98*, 255–262. [CrossRef]

11. Mortensen, A.B.; Sorensen, S.E. Relationship between Boar Taint and Skatole Determined with a New Analysis Method. In Proceedings of the 32nd European Meeting Research Workers, Graz, Austria, 18–19 October 1984; pp. 394–396.
12. Burgeon, C.; Debliquy, M.; Lahem, D.; Rodriguez, J.; Ly, A.; Fauconnier, M.L. Past, Present, and Future Trends in Boar Taint Detection. *Trends Food Sci. Technol.* **2021**, *112*, 283–297. [[CrossRef](#)]
13. Lund, B.W.; Borggaard, C.; Birkler, R.I.D.; Jensen, K.; Støier, S. High Throughput Method for Quantifying Androstenone and Skatole in Adipose Tissue from Uncastrated Male Pigs by Laser Diode Thermal Desorption-Tandem Mass Spectrometry. *Food Chem. X* **2021**, *9*, 100113. [[CrossRef](#)]
14. Verplanken, K.; Stead, S.; Jandova, R.; Van Poucke, C.; Claereboudt, J.; Bussche, J.V.; De Saeger, S.; Takats, Z.; Wauters, J.; Vanhaecke, L. Rapid Evaporative Ionization Mass Spectrometry for High-Throughput Screening in Food Analysis: The Case of Boar Taint. *Talanta* **2017**, *169*, 30–36. [[CrossRef](#)]
15. Sørensen, K.M.; Westley, C.; Goodacre, R.; Engelsen, S.B. Simultaneous Quantification of the Boar-Taint Compounds Skatole and Androstenone by Surface-Enhanced Raman Scattering (SERS) and Multivariate Data Analysis. *Anal. Bioanal. Chem.* **2015**, *407*, 7787–7795. [[CrossRef](#)]
16. Liu, X.; Schmidt, H.; Mörlein, D. Feasibility of Boar Taint Classification Using a Portable Raman Device. *Meat Sci.* **2016**, *116*, 133–139. [[CrossRef](#)] [[PubMed](#)]
17. Verplanken, K.; Wauters, J.; Van Durme, J.; Claus, D.; Vercammen, J.; De Saeger, S.; Vanhaecke, L. Rapid Method for the Simultaneous Detection of Boar Taint Compounds by Means of Solid Phase Microextraction Coupled to Gas Chromatography/Mass Spectrometry. *J. Chromatogr. A* **2016**, *1462*, 124–133. [[CrossRef](#)] [[PubMed](#)]
18. Burgeon, C.; Markey, A.; Debliquy, M.; Lahem, D.; Rodriguez, J.; Ly, A.; Fauconnier, M.-L. Comprehensive SPME-GC-MS Analysis of VOC Profiles Obtained Following High-Temperature Heating of Pork Back Fat with Varying Boar Taint Intensities. *Foods* **2021**, *10*, 1311. [[CrossRef](#)] [[PubMed](#)]
19. Rius, M.A.; Hortós, M.; García-Regueiro, J.A. Influence of Volatile Compounds on the Development of Off-Flavours in Pig Back Fat Samples Classified with Boar Taint by a Test Panel. *Meat Sci.* **2005**, *71*, 595–602. [[CrossRef](#)]
20. Psillakis, E.; Yiantzi, E.; Sanchez-Prado, L.; Kalogerakis, N. Vacuum-Assisted Headspace Solid Phase Microextraction: Improved Extraction of Semivolatiles by Non-Equilibrium Headspace Sampling under Reduced Pressure Conditions. *Anal. Chim. Acta* **2012**, *742*, 30–36. [[CrossRef](#)] [[PubMed](#)]
21. 3-Methylindole, C9H9N–PubChem. Available online: <https://pubchem.ncbi.nlm.nih.gov/compound/3-Methylindole#section=Structures> (accessed on 7 October 2023).
22. 5alpha-Androst-16-En-3-One, C19H28O–PubChem. Available online: <https://pubchem.ncbi.nlm.nih.gov/compound/6852393#section=Structures> (accessed on 7 October 2023).
23. Dansyl Hydrazine, C12H15N3O2S–PubChem. Available online: <https://pubchem.ncbi.nlm.nih.gov/compound/94442#section=2D-Structure> (accessed on 8 October 2023).
24. Hogard, M.L.; Lunte, C.E.; Lunte, S.M. Detection of Reactive Aldehyde Biomarkers in Biological Samples Using Solid-Phase Extraction Pre-Concentration and Liquid Chromatography with Fluorescence Detection. *Anal. Methods* **2017**, *9*, 1848–1854. [[CrossRef](#)]
25. Hansen-Møller, J. Rapid High-Performance Liquid Chromatographic Method for Simultaneous Determination of Androstenone, Skatole and Indole in Back Fat from Pigs. *J. Chromatogr. B Biomed. Sci. Appl.* **1994**, *661*, 219–230. [[CrossRef](#)]
26. Paquot, C. Standard Methods for the Analysis of Oils, Fats and Derivatives. *Pure Appl. Chem.* **1982**, *54*, 233–246. [[CrossRef](#)]
27. Burgeon, C.; Font-i-Furnols, M.; Garrido, M.D.; Linares, M.B.; Brostaux, Y.; Sabeña, G.; Fauconnier, M.-L.; Panella-Riera, N. Can Sensory Boar Taint Levels Be Explained by Fatty Acid Composition and Emitted Volatile Organic Compounds in Addition to Androstenone and Skatole Content? *Meat Sci.* **2022**, *195*, 108985. [[CrossRef](#)] [[PubMed](#)]
28. Bekaert, K.M.; Aluwé, M.; Vanhaecke, L.; Heres, L.; Duchateau, L.; Vandendriessche, F.; Tuytens, F.A.M. Evaluation of Different Heating Methods for the Detection of Boar Taint by Means of the Human Nose. *Meat Sci.* **2013**, *94*, 125–132. [[CrossRef](#)] [[PubMed](#)]
29. Mörlein, D.; Tholen, E. Fatty Acid Composition of Subcutaneous Adipose Tissue from Entire Male Pigs with Extremely Divergent Levels of Boar Taint Compounds—An Exploratory Study. *Meat Sci.* **2015**, *99*, 1–7. [[CrossRef](#)]
30. Oleic Acid, C18H34O2–PubChem. Available online: <https://pubchem.ncbi.nlm.nih.gov/compound/Oleic-acid#section=Vapor-Pressure> (accessed on 14 April 2021).
31. Palmitic Acid, C16H32O2–PubChem. Available online: <https://pubchem.ncbi.nlm.nih.gov/compound/985#section=2D-Structure> (accessed on 8 October 2023).
32. Linoleic Acid, C18H32O2–PubChem. Available online: <https://pubchem.ncbi.nlm.nih.gov/compound/5280450#section=2D-Structure> (accessed on 8 October 2023).
33. Zamaratskaia, G.; Gilmore, W.J.; Lundström, K.; Squires, E.J. Effect of Testicular Steroids on Catalytic Activities of Cytochrome P450 Enzymes in Porcine Liver Microsomes. *Food Chem. Toxicol.* **2007**, *45*, 676–681. [[CrossRef](#)]
34. Bonneau, M. Use of Entire Males for Pig Meat in the European Union. *Meat Sci.* **1998**, *49*, 257–272. [[CrossRef](#)]
35. Whittington, F.M.; Zammerini, D.; Nute, G.R.; Baker, A.; Hughes, S.I.; Wood, J.D. Comparison of Heating Methods and the Use of Different Tissues for Sensory Assessment of Abnormal Odours (Boar Taint) in Pig Meat. *Meat Sci.* **2011**, *88*, 249–255. [[CrossRef](#)]
36. Trautmann, J.; Meier-Dinkel, L.; Gertheiss, J.; Mörlein, D. Boar Taint Detection: A Comparison of Three Sensory Protocols. *Meat Sci.* **2016**, *111*, 92–100. [[CrossRef](#)]

37. Hansson, K.E.; Lundstrom, K.; Fjellkner-Modig, S.; Persson, J. The Importance of Androstene and Skatole for Boar Taint. *Swedish J. Agric. Res.* **1980**, *10*, 167–173.
38. Rius, M.A.; García-Regueiro, J.A. Skatole and Indole Concentrations in Longissimus Dorsi and Fat Samples of Pigs. *Meat Sci.* **2001**, *59*, 285–291. [[CrossRef](#)]
39. Shirey, R.E. SPME Commercial Devices and Fibre Coatings. In *Handbook of Solid Phase Microextraction*; Elsevier Inc.: Amsterdam, The Netherlands, 2012; pp. 99–133. ISBN 9780124160170.
40. Serra, A.; Buccioni, A.; Rodriguez-Estrada, M.T.; Conte, G.; Cappucci, A.; Mele, M. Fatty Acid Composition, Oxidation Status and Volatile Organic Compounds in “Colonnata” Lard from Large White or Cinta Senese Pigs as Affected by Curing Time. *Meat Sci.* **2014**, *97*, 504–512. [[CrossRef](#)] [[PubMed](#)]
41. Domínguez, R.; Pateiro, M.; Gagaoua, M.; Barba, F.J.; Zhang, W.; Lorenzo, J.M. A Comprehensive Review on Lipid Oxidation in Meat and Meat Products. *Antioxidants* **2019**, *8*, 429. [[CrossRef](#)]
42. Moldoveanu, S.C. Pyrolysis of Amino Acids and Small Peptides. In *Techniques and Instrumentation in Analytical Chemistry*; Elsevier Inc.: Amsterdam, The Netherlands, 2010; Volume 28, pp. 527–578. ISBN 9780444531131.
43. Methyl Stearate, C19H38O2–PubChem. Available online: <https://pubchem.ncbi.nlm.nih.gov/compound/Methyl-Stearate#section=Vapor-Pressure> (accessed on 9 October 2023).
44. Mascrez, S.; Psillakis, E.; Purcaro, G. A Multifaceted Investigation on the Effect of Vacuum on the Headspace Solid-Phase Microextraction of Extra-Virgin Olive Oil. *Anal. Chim. Acta* **2020**, *1103*, 106–114. [[CrossRef](#)] [[PubMed](#)]
45. Mathur, P.K.; ten Napel, J.; Bloemhof, S.; Heres, L.; Knol, E.F.; Mulder, H.A. A Human Nose Scoring System for Boar Taint and Its Relationship with Androstene and Skatole. *Meat Sci.* **2012**, *91*, 414–422. [[CrossRef](#)]
46. Bonneau, M.; Walstra, P.; Claudi-Magnussen, C.; Kempster, A.J.; Tornberg, E.; Fischer, K.; Diestre, A.; Siret, F.; Chevillon, P.; Claus, R.; et al. An International Study on the Importance of Androstene and Skatole for Boar Taint: IV. Simulation Studies on Consumer Dissatisfaction with Entire Male Pork and the Effect of Sorting Carcasses on the Slaughter Line, Main Conclusions and Recommendations. *Meat Sci.* **2000**, *54*, 285–295. [[CrossRef](#)]
47. Papadopoulou, O.S.; Tassou, C.C.; Schiavo, L.; Nychas, G.-J.E.; Panagou, E.Z. Rapid Assessment of Meat Quality by Means of an Electronic Nose and Support Vector Machines. *Procedia Food Sci.* **2011**, *1*, 2003–2006. [[CrossRef](#)]
48. van Gemert, L.J. *Flavour Thresholds—Compilations of Flavour Threshold Values in Water and Other Media*; Oliemans Punter & Partners BV: Utrecht, The Netherlands, 2011.
49. Aaslyng, M.D.; Meinert, L. Meat Flavour in Pork and Beef—From Animal to Meal. *Meat Sci.* **2017**, *132*, 112–117. [[CrossRef](#)]
50. Han, D.; Zhang, C.H.; Fauconnier, M.L.; Jia, W.; Wang, J.F.; Hu, F.F.; Xie, D.W. Characterization and Comparison of Flavor Compounds in Stewed Pork with Different Processing Methods. *Lwt* **2021**, *144*, 111229. [[CrossRef](#)]
51. Font-i-Furnols, M.; Martín-bernal, R.; Aluwé, M.; Bonneau, M.; Haugen, J.E.; Mörlein, D.; Mörlein, J.; Panella-riera, N.; Škrlep, M. Feasibility of on/at Line Methods to Determine Boar Taint and Boar Taint Compounds: An Overview. *Animals* **2020**, *10*, 1886. [[CrossRef](#)]

Disclaimer/Publisher’s Note: The statements, opinions and data contained in all publications are solely those of the individual author(s) and contributor(s) and not of MDPI and/or the editor(s). MDPI and/or the editor(s) disclaim responsibility for any injury to people or property resulting from any ideas, methods, instructions or products referred to in the content.